ELSEVIER

Engineering Geology 63 (2002) 301–331

ENGINEERING GEOLOGY

www.elsevier.com/locate/enggeo

The mobility of long-runout landslides

François Legros[1]

Institute of Earth Sciences "Jaume Almera", Consejo Superior de Investigaciones Científicas, C\Lluís Solé i Sabarís s/n, 08028 Barcelona, Spain

Received 6 June 2000; accepted 22 August 2001

Abstract

Several issues relevant to the mobility of long-runout landslides are examined. A central idea developed in this paper is that the apparent coefficient of friction (ratio of the fall height to the runout distance) commonly used to describe landslide mobility is physically meaningless. It is proposed that the runout distance depends primarily on the volume and not on the fall height, which just adds scatter to the correlation. The negative correlation observed between the apparent coefficient of friction and the volume is just due to the fact that, on the gentle slopes on which landslides travel and come to rest, a large increase in runout distance due to a large volume corresponds to a small increase in the total fall height, hence to a decrease in the apparent coefficient of friction. It is shown that the spreading of a fluid-absent, granular flow is not able to explain the large runout distances of landslides, and in particular does not allow the centre of mass to travel further than expected for a sliding block. This contrasts with the behaviour of natural landslides, for which the centre of mass is shown to travel much further than expected from a simple Coulomb model. The presence of an interstitial fluid which can partly or entirely support the load of particles allows the effective coefficient of solid friction to be reduced or even suppressed. Air is not efficient for fluidising large landslides and a loose debris cannot slide over a basal layer of entrapped and compressed air, as air would rapidly pass through the debris in the form of bubbles during batch sedimentation. Water is much more efficient as a fluidising medium due to its higher density and viscosity, and its incompressibility. As water is known to enhance the mobility of the saturated debris flows, it is proposed that water is also responsible for the long runout of landslides. This is consistent with the fact that the increase in runout with volume is similar for debris flows and landslides. Field evidence suggests that most landslides are unsaturated with water but not dry, even on Mars. Comparison of the velocity of well-documented landslides with that predicted by fluid-absent, granular models shows that these models predict landslides that are much faster and less responsive to topography than natural ones. The relatively low velocities of landslides suggest that energy dissipation is dominated by a velocity-dependent stress and that the coefficient of solid friction is very low. This is consistent with the physics of fluidised or partly fluidised debris and suggests that landslide velocity may be controlled by local slope and flow thickness rather than by the initial fall height. In the absence of a supply of fluid at the base, fluidisation requires a net downward flux of sediment, implying some deposition at the base of landslides, which may thus progressively run out of material. In such a model, the spreading of the portion of a landslide beyond a certain distance would primarily depend on the volume passing this distance and not on the total volume of the landslide. Landslide deposits may therefore have self-similar shapes, in which the area covered beyond a certain distance is a constant function of the volume beyond that distance. It is shown that the shape of some well-documented landslide deposits is in reasonable agreement with this prediction. One consequence is that, as recently proposed for debris flows, assessment of hazards related to landslides should

E-mail address: f_legros@yahoo.com (F. Legros).

[1] Current address: Urb. San Isidro F1, Vallecito, Arequipa, Peru.

0013-7952/02/$ - see front matter
PII: S0013-7952(01)00090-4

be based on the correlation between the volume and the area covered by the deposit, rather than on the apparent coefficient of friction. © 2002 Published by Elsevier Science B.V.

Keywords: Landslide; Debris flow; Granular flow; Pore pressure

1. Introduction

Long-runout landslides are common geological features in a variety of environments. Their deposits are found in volcanic and non-volcanic terrains, subaerial and submarine settings, and even on Mars and on the Moon. Their volumes range from 10^5 to 10^{11} m^3 in terrestrial, subaerial settings, and up to 10^{13} m^3 for submarine and extraterrestrial landslides. A defining characteristic of long-runout landslides is that they travel further than expected from simple frictional models. This high mobility, which makes these phenomena very hazardous, was first noted by Heim (1932) and has much intrigued geologists since.

Many hypotheses have been put forward to explain the long runout of landslides. They are briefly summarised below but the reader is also referred to the review by Shaller and Smith-Shaller (1996). Several hypotheses have invoked the presence of a fluidising medium such as air, water, vapour, volcanic gases or a suspension of fine particles. Kent (1966) proposed that entrapped air could fluidise landslides. Shreve (1968a,b) and Fahnestock (1978) suggested that a cushion of entrapped air would support landslides rather than fluidise them. Hsü (1975) hypothesised that the fine particles alone, without the help of a supporting fluid, could fluidise the coarser, moving debris. In some specific volcanic landslides, fluidisation by volcanic gases has been proposed (Voight et al., 1983). Goguel (1978) showed that vaporisation of water at the base of landslides could produce pore pressure in excess of lithostatic and thus strongly reduce friction. Johnson (1978) and Voight and Sousa (1994) presented evidence for the presence of a water-saturated base in, respectively, the Blackhawk and the Ontake-san landslides, and proposed an emplacement mechanism similar to that of debris flows. At the opposite, some authors have attempted to explain landslide mobility with fluid-absent, granular models. The proposed hypotheses include acoustic fluidisation (Melosh, 1979), spreading of a rapid granular flow (Davies, 1982; Straub, 1997), self-lubrication (Campbell, 1989; Cleary and Campbell, 1993; Straub, 1996), and spreading of a granular flow in a regime transitional between frictional and collisional (Campbell et al., 1995). The mobility of landslides has also been considered using continuum models with bulk rheological properties such as viscosity and yield strength, without specific assumptions about the microscopic physics (e.g., Voight et al., 1983; McEwen and Malin, 1989; McEwen, 1989; Dade and Huppert, 1998; Takarada et al., 1999). Models which take into account changes of mass due to deposition or bulking have also been offered (Cannon and Savage, 1988; Van Gassen and Cruden, 1989; Voight and Sousa, 1994; Hungr and Evans, 1997). While many of the mechanisms invoked may have been important in some specific landslide events, none of them has been widely recognised as a universal explanation for landslide mobility, and the debate continues.

This paper re-examines several important issues regarding landslide mobility, including the relationships between volume, area, runout distance, fall height, and apparent coefficient of friction for landslides in different environments, the possible role of air, water or particle suspension as a fluidising medium on the Earth, Mars and the Moon, the ability of fluid-absent, granular models to explain landslide mobility, the velocity of landslides and the control exerted by topography, and the mass distribution and thickness profile in the deposits.

2. Relationships between fall height, runout distance, area and volume

2.1. Uncertainties on the data

Before examining the general relationships between landslide fall height, runout distance, area and volume, it is useful to wonder whether the estimates of these variables are not biased and whether they are accurate enough. The volume of landslide is generally estimated by multiplying the area covered by the deposit

by an estimated average thickness. Area as well as length is likely to be estimated fairly accurately, even for submarine or extraterrestrial deposits. In contrast, thickness is often well constrained at the distal end of the deposit only. Young landslide deposits have seldom been sufficiently dissected to offer cross-sections down to their base and the unknown previous topography makes it difficult to estimate the volume. For old landslide deposits where erosion has been important, the volume lost can be difficult to estimate. When there is some uncertainty, most authors choose to present minimum estimates. As thickness tends to decrease with distance from source, volumes extrapolated from the distal thickness are likely to be underestimates. For some landslides on Mars, multiplying the distal thickness by the area yields volume estimates up to one order of magnitude less than the volume of the corresponding scar (McEwen, 1989). On the Earth, we may expect that field control allows more accurate volume estimates. As the volumes of long-runout landslides cover a wide range from 10^5 to 10^{13} m^3, an uncertainty generally much less than one order of magnitude is acceptable for the purpose of investigating the effect of volume on mobility.

2.2. Translation of the centre of mass

Data available on the distance travelled by landslides usually consist of the runout distance, L_{max}, and the total drop height, H_{max} (Fig. 1). These are the easiest parameters to measure and they are probably estimated with less than 20% of relative error in most cases. However, in many physical analyses of landslide emplacement, the parameters of interest are not H_{max} and L_{max} but H and L, the height lost and distance travelled by the centre of mass. One particularly interesting question is whether the low apparent friction coefficient computed for many landslides is not simply due to the fact that H_{max}/L_{max} is considered instead of H/L. This is essentially the idea of Davies (1982), who suggested that the low H_{max}/L_{max} ratios observed were due to landslide spreading with a "normal" coefficient of friction, represented by H/L.

There are few deposits for which H and L have been estimated, but, nevertheless, for any landslide deposit of known H_{max} and L_{max}, we can test Davies' hypothesis by calculating the thickness profile necessary for H/L to be equal to the "normal" coefficient of friction (~ 0.6). For example, for large landslides which have typical H_{max}/L_{max} ratios of about 0.1, L should be about one sixth of L_{max} in order to get an H/L ratio of about 0.6, if we consider that $H \sim H_{max}$. One may consider several simple geometries (Fig. 2). For a deposit confined in a channel with vertical walls, a linear decrease of thickness with distance from source would yield $L = L_{max}/3$. Assuming an exponential thinning, the condition $L = L_{max}/6$ would be obtained for a deposit more than 100 times thicker at its proximal end than at its distal end. For unconfined, radially spread deposits, the width of the deposit increases with distance from source and L tends to be closer to L_{max} than for the two-dimensional case.

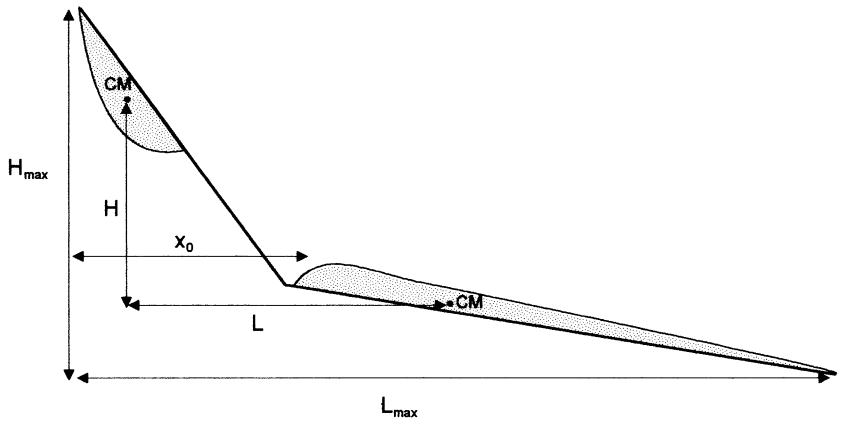

Fig. 1. Sketch of landslide deposit and failing mass and definition of the parameters x_0, H, L, H_{max} and L_{max} used in this paper. CM indicates the centre of mass of the failing mass and the deposit.

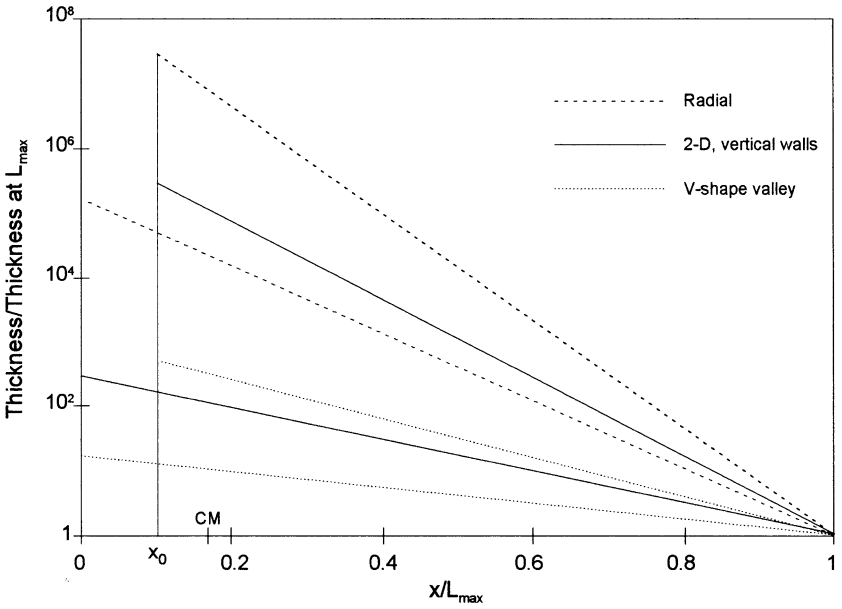

Fig. 2. Thickness of a landslide deposit such that the centre of mass (CM) is at a distance $L=L_{max}/6$ from the origin, assuming an exponential thickness profile and three simple geometries: a radially spread deposit, a deposit channelled in a valley with vertical walls (2D case) and a deposit in a V-shape valley. Thickness profiles are presented for the case where the deposit starts from the origin and for the more typical case where there is a distance $x_0=L_{max}/10$ between the origin and the proximal end of the deposit. Natural landslide deposits do not show such high thinning rates and proximal thicknesses, suggesting that $L>>L_{max}/6$ for most of them and so that landslides with $H_{max}/L_{max}\leq 0.1$ have $H/L<<0.6$.

The condition $L=L_{max}/6$ therefore requires a greater exponential thinning rate, with a proximal end of the deposit up to 10^5 times thicker than the distal end. (Note that, for a radially spread deposit, strictly the concept of distance of the centre of mass becomes meaningless, as it is clear that the centre of mass of an hypothetical deposit extending over 360° would be at its origin. Instead, L is the average distance travelled.) Deposits channelled in V-shape valleys may have a width which decreases with distance from source, as their width would be proportional to their thickness. It can be shown that for a linear decrease of thickness, such deposits would have $L=L_{max}/4$. Assuming exponential thinning, the condition $L=L_{max}/6$ would be attained for a deposit 20 times thicker at its proximal end than at its distal end.

In practice, there is often a significant distance between the origin and the proximal end of the deposit (x_0), and/or the maximum thickness of deposit does not occur at the proximal end (Fig. 1). Table 1 shows that, for well-documented landslide deposits, x_0 is generally greater than $L_{max}/10$. For $x_0=L_{max}/10$, Fig. 2 shows that, in order to maintain $L=L_{max}/6$, the thinning rate and hence the proximal thickness of deposit must still be higher, and this conclusion should hold whatever the exact shape of the deposit. Such very high proximal thicknesses (more than 100 times the distal thicknesses for the most favourable geometry) are not typical of landslide deposits. Moreover, in some landslides, the thickness of the proximal deposit is artificially increased by the accumulation of material from less mobile pulses during multiple retrogressive failure (e.g., at Mount St. Helens, Voight et al., 1983). In some cases, the distance x_0 is even greater than the theoretical distance L for a friction coefficient of 0.6, which means that the whole deposit lies beyond the distance predicted for its centre of mass by a simple frictional model. This occurs for the Blackhawk landslide deposit, which lies between 2 and 9 km from its origin, while, in order to get $H/L=0.6$, L should be less than 2 km (Johnson, 1978). From Johnson's data, L can be estimated to be about 6 km, only 1.5 times less than L_{max}. The same occurs for the giant Mount Shasta landslide (Crandell, 1988),

Table 1
Comparison between H/L and H_{max}/L_{max} for several landslide deposits

	L_{max} (km)	H_{max}/L_{max}	L (km)	H/L	V (km^3)	x_0/L_{max}
Blackhawk (1)	9	0.13	5–6[a]	0.20–0.17[a]	0.3	0.22
Elm (2)	2	0.3	0.8–1[a]	0.42	0.01	0.25
Lastarria (3)	6.7	0.15	3–4[a]	0.20–0.15[a]	0.09	0.3[a]
Mount St. Helens (4)	23	0.09	8–12[a]	0.25–0.12[a]	2.8	0.2[a]
Nevado de Colima (5)	120	0.04	30–50[a]	0.13–0.06[a]	22–33	0.04[a]
Shasta (6)	49	0.07	20–30[a]	0.15–0.07[a]	45	0.16[a]
Sherman (7)	6	0.22	3–4[a]	0.19	0.01	0.16[a]

References are as follows: (1) Johnson (1978), (2) Hsü (1975), (3) Naranjo and Francis (1987), (4) Voight et al. (1983), (5) Stoopes and Sheridan (1992), (6) Crandell (1988), (7) McSaveney (1978). H_{max}, L_{max}, H, L, and x_0 are defined in Fig. 1.
[a] Estimated in this paper.

where x_0 ($\sim$10 km) is much greater than $H/0.6$ ($\sim$5 km). Subdivision of the deposit by Crandell in seven areas, each with an estimated mean thickness, allows us to estimate a mean travelled distance L of about 27 km, only two times less than L_{max}.

In the above calculations, it was assumed that H was equal to H_{max}. In fact, the drop height measured from the distance L is always less than that measured from the distal end of the deposit. In addition, we should consider the centre of mass of the failing block rather than its highest point, so H is likely to be significantly less than H_{max}, so as to substantially reduce H/L. For a few well-documented deposits, H/L can be estimated with some confidence (Table 1). For example, Naranjo and Francis (1987) describe a landslide at Lastarria volcano (Chile) with $H_{max} \sim 1$ km and $L_{max} \sim 6.7$ km. From their data, the drop height of the centre of mass can be estimated to 0.6 km and the average travelled distance to 3–4 km, which suggests that H_{max}/L_{max} ($\sim$0.15) is actually a good estimate for H/L (0.15–0.20) in this case. In the case of the Blackhawk landslide, the ratio H/L is about 0.20–0.17, not dramatically higher than H_{max}/L_{max} ($\sim$0.13). For the Elm landslide, Hsü (1975) reports $H_{max}/L_{max} \sim 0.3$ and $H/L \sim 0.42$, while for the Sherman landslide, McSaveney (1978) estimates that H/L ($\sim$0.19) is in fact less than H_{max}/L_{max} ($\sim$0.22). Therefore, there seems to have little doubt that, for most landslides, the low H_{max}/L_{max} ratio cannot be explained by frictional spreading of the mass with a normal friction coefficient. Instead, the centre of mass does travel further than predicted by a frictional model with a normal friction coefficient, and travels further for larger landslides. This last point can be illustrated by the giant landslide of Nevado de Colima, which travelled 120 km before entering the Pacific Ocean, with an estimated H_{max}/L_{max} of about 0.04 (Stoopes and Sheridan, 1992). If we estimate conservatively that the centre of mass travelled only 35 km, we still have an H/L ratio of about 0.1, lower than the H/L and even H_{max}/L_{max} ratios observed for most small landslides. A similar value of H/L is found for the giant landslide of Mount Shasta (Table 1).

2.3. Dependence of runout on fall height and volume

It is well known that, when data from many landslides (Table 2) are plotted in a graph of H_{max}/L_{max} versus volume, the ratio H_{max}/L_{max} shows a tendency to decrease with increasing volume, from a value of about 0.6, expected for a purely frictional slide, at volumes smaller than 10^5 m^3, to values lower than 0.1 for volumes in excess of 1 km^3 (Fig. 3a). Although unquestionable, this trend shows a large scatter. Davies (1982) proposed that the actual runout of a landslide is essentially controlled by its spreading, hence by its volume. He showed that a plot of runout versus volume gives a better correlation (Fig. 3b; Table 3), and suggested that drop height is of secondary importance and just adds scatter to the correlation. In a set of experiments using bentonite as an analogue material for landslides, Hsü (1975) showed that the height from which a given volume was released had no influence on the runout distance and total area of the final deposit, which were only dependent on the volume. There is an additional reason to question the physical significance of the H_{max}/L_{max} or H/L ratio. The use of this

Table 2
Estimated volume (V), runout distance (L_{max}), fall height (H_{max}), area (A) and apparent coefficient of friction (H_{max}/L_{max}) for 203 landslide and debris-flow deposits in a variety of environments

	V (km^3)	L_{max} (km)	H_{max} (km)	A (km^2)	H_{max}/L_{max}	References
Subaerial non-volcanic landslides						
Blackhawk	0.28	9.6	1.2		0.125	Hayashi and Self (1992)
Corno di desde	0.02	3.7	1.2		0.324	Hayashi and Self (1992)
Deyen, Glarus	0.6	6.6	0.74		0.112	Hayashi and Self (1992)
Diablerets	0.05	5.5	1.9		0.345	Hayashi and Self (1992)
Disentis	0.015	2.1	0.74		0.352	Hayashi and Self (1992)
Elm	0.01	2.3	0.71		0.309	Hayashi and Self (1992)
Engelberg	2.75	7.4	1.6		0.216	Hayashi and Self (1992)
Fernpass	1	15.6	1.4		0.090	Hayashi and Self (1992)
Flims	12	15.6	2		0.128	Hayashi and Self (1992)
Frank	0.03	3.5	0.87		0.249	Hayashi and Self (1992)
Garnish	0.8	7.5	1.9		0.253	Hayashi and Self (1992)
Goldau	0.035	6	1.2		0.200	Hayashi and Self (1992)
Gros Ventre	0.038	3.4	0.56		0.165	Hayashi and Self (1992)
Kandertal	0.14	9.9	1.9		0.192	Hayashi and Self (1992)
Maligne Lake	0.5	5.47	0.92		0.168	Hayashi and Self (1992)
Medicine Lake	0.086	1.22	0.32		0.262	Hayashi and Self (1992)
Madison	0.029	1.6	0.43		0.269	Hayashi and Self (1992)
Mombiel	0.0008	0.8	0.37		0.463	Hayashi and Self (1992)
Obersee GL	0.12	5	1.8		0.360	Hayashi and Self (1992)
Pamir	2	6.2	1.5		0.242	Hayashi and Self (1992)
Poshivo	0.15	4.1	1.5		0.366	Hayashi and Self (1992)
Saidmarreh	20	18.9	1.5		0.079	Hayashi and Self (1992)
Schächental	0.0005	3.1	1.8		0.581	Hayashi and Self (1992)
Scimada Saoseo	0.08	5.5	1.5		0.273	Hayashi and Self (1992)
Sherman	0.03	6.2	1.3		0.210	Hayashi and Self (1992)
Siders	1.5	17.4	2.4		0.138	Hayashi and Self (1992)
Tamins	1.3	13.5	1.3		0.096	Hayashi and Self (1992)
Vaiont	0.25	1.5	0.5		0.333	Hayashi and Self (1992)
Val Lagone	0.00065	2.4	1.05		0.438	Hayashi and Self (1992)
Voralpsee	0.03	3.4	1.1		0.324	Hayashi and Self (1992)
Wengen 1	0.0025	1.1	0.5		0.455	Hayashi and Self (1992)
Wengen 2	0.0055	1.4	0.59		0.421	Hayashi and Self (1992)
Subaerial volcanic landslides						
Akagi	4	19	2.4		0.126	Hayashi and Self (1992)
Asakusa	0.04	6.5	1		0.154	Hayashi and Self (1992)
Asama	2	20	1.8	90[a]	0.090	Hayashi and Self (1992)
Bandai-san 1888	1.5	11	1.2	34[a]	0.109	Hayashi and Self (1992)
Bezymianni 1956	0.8	18	2.4	30[a]	0.133	Hayashi and Self (1992)
Callaqui	0.15	15	3.1		0.207	Hayashi and Self (1992)
Chaos Crags	0.15	5	0.65	8[a]	0.130	Hayashi and Self (1992)
Chimborazo	8.1	35	3.6		0.103	Hayashi and Self (1992)
Chokai	3.5	25	2.2		0.088	Hayashi and Self (1992)
Colima	12.5	40	4	900[a]	0.100	Hayashi and Self (1992)
Egmont (Pungarehu)	7.5	31	2.6	250[a]	0.084	Hayashi and Self (1992)
Egmont (Opua)	0.35	27	2.5	120[a]	0.093	Hayashi and Self (1992)
Fuji	1.8	24	2.5		0.104	Hayashi and Self (1992)
Galunggung	2.9	25	1.9	175[a]	0.076	Hayashi and Self (1992)
Iriga	1.5	11	1.05	65[a]	0.095	Hayashi and Self (1992)
Iwaki	1.3	14	1.6		0.114	Hayashi and Self (1992)
Komagatake	0.25	11.5	1		0.087	Hayashi and Self (1992)

Table 2 (*continued*)

	V (km^3)	L_{max} (km)	H_{max} (km)	A (km^2)	H_{max}/L_{max}	References
Subaerial volcanic landslides						
Kurohime	0.12	6	0.8		0.133	Hayashi and Self (1992)
Mageik	0.09	9	0.8		0.089	Hayashi and Self (1992)
Mawenzi	7.1	60	4.5	1150[a]	0.075	Hayashi and Self (1992)
Meru	15	50	3.9	1400[a]	0.078	Hayashi and Self (1992)
Monbacho	1	12	1.3	45[a]	0.108	Hayashi and Self (1992)
Mt. St. Helens 1980	2.5	24	2.55	60[a]	0.106	Hayashi and Self (1992)
Myoko (Sekikawa)	0.8	19	2		0.105	Hayashi and Self (1992)
Myoko (Taguchi)	0.23	8	1.4	10[a]	0.175	Hayashi and Self (1992)
Ovalnaya Zimina	0.4	17	2.4		0.141	Hayashi and Self (1992)
Papandayan	0.14	11	1.5		0.136	Hayashi and Self (1992)
Peteroa	16	85	3.9		0.046	Hayashi and Self (1992)
Popa	0.8	11	1.2		0.109	Hayashi and Self (1992)
Popocatepetl	28	33	4		0.121	Hayashi and Self (1992)
Shasta	26	50	3.55	450[a]	0.071	Hayashi and Self (1992)
Shiveluch	1.5	12	2	98[a]	0.167	Hayashi and Self (1992)
Sierra Velluda	0.5	25	3.4		0.136	Hayashi and Self (1992)
Socompa	17	35	3.25	480[a]	0.093	Hayashi and Self (1992)
Tashiro	0.55	8.8	0.7		0.080	Hayashi and Self (1992)
Tateshina	0.35	12.5	1.4		0.112	Hayashi and Self (1992)
Unzen	0.34	6.5	0.85	12[a]	0.131	Hayashi and Self (1992)
Usu	0.3	6.5	0.5		0.077	Hayashi and Self (1992)
Yatsugatake (Nirasaki)	9	32	2.4		0.075	Hayashi and Self (1992)
Yatsugatake (Otsukigawa)	0.27	12.5	1.4		0.112	Hayashi and Self (1992)
Soufrière Guadeloupe	0.5	9.5	1.35	25	0.142	Siebert (1984)
St. Helens 20000 BP	1	16	1.75		0.109	Siebert (1984)
Vesuvius 1944	0.000179	0.64	0.575	0.022	0.898	Hazlett et al. (1991)
Vesuvius 1944	0.0009	0.94	0.505	0.113	0.537	Hazlett et al. (1991)
Vesuvius 1944	0.00055	0.5	0.285	0.099	0.570	Hazlett et al. (1991)
Vesuvius 1944	0.000793	0.96	0.47	0.126	0.490	Hazlett et al. (1991)
Vesuvius 1944	0.001	1.24	0.636	0.136	0.513	Hazlett et al. (1991)
Vesuvius 1944	0.0011	0.68	0.36	0.145	0.529	Hazlett et al. (1991)
Vesuvius 1944	0.00116	0.82	0.41	0.161	0.500	Hazlett et al. (1991)
Jocotitlán	2.8	12	1.15	80	0.110	Siebe et al. (1992)
Submarine landslides						
Grant Banks	76	110	0.365		0.003	Hampton et al. (1996)
Hawaii		160	2		0.013	Hampton et al. (1996)
Kidnappers	8	11	0.05		0.005	Hampton et al. (1996)
Bay of Biscay		21	0.25		0.012	Hampton et al. (1996)
Rockall	300	160	0.33		0.002	Hampton et al. (1996)
Bassein		37	0.36		0.010	Hampton et al. (1996)
Agulhas		106	0.375		0.004	Hampton et al. (1996)
Copper River delta		18	0.115		0.006	Hampton et al. (1996)
Albatross Bank		5.3	0.3		0.057	Hampton et al. (1996)
Portlock Bank		6.5	0.2		0.031	Hampton et al. (1996)
Kayak trough		15	0.115		0.008	Hampton et al. (1996)
Atlantic Coast		3.4	0.03		0.009	Hampton et al. (1996)
		4.8	0.08		0.017	Hampton et al. (1996)
		2.3	0.018		0.008	Hampton et al. (1996)
Magdalena	0.3	24	1.4		0.058	Hampton et al. (1996)
Valdez	0.075	1.28	0.168		0.131	Hampton et al. (1996)

(*continued on next page*)

Table 2 (*continued*)

	V (km^3)	L_{max} (km)	H_{max} (km)	A (km^2)	H_{max}/L_{max}	References
Submarine landslides						
Mississippi River delta	0.04		0.02			Hampton et al. (1996)
Suva	0.15		0.1			Hampton et al. (1996)
Scripps Canyon	0.00005		0.006			Hampton et al. (1996)
Orkdalsfjord	0.025	22.5	0.5		0.022	Hampton et al. (1996)
Sandnesjoen	0.005	1.2	0.18		0.150	Hampton et al. (1996)
Sokkelvik	0.0005	2.5	0.12		0.048	Hampton et al. (1996)
Helsinki	0.000006	0.4	0.011		0.028	Hampton et al. (1996)
Storegga	800	160	1.7		0.011	Hampton et al. (1996)
Typical Atlantic Ocean		4	1.2		0.300	Hampton et al. (1996)
Cape Fear		30	0.7		0.023	Hampton et al. (1996)
Blake Escarpment	600	42	3.6		0.086	Hampton et al. (1996)
East Break East	13	70	1.15		0.016	Hampton et al. (1996)
East Break West	160	110	1.1		0.010	Hampton et al. (1996)
Navarin Canyon	5	6	0.175		0.029	Hampton et al. (1996)
Seward	0.0027	3	0.2		0.067	Hampton et al. (1996)
Alsek		2	0.02		0.010	Hampton et al. (1996)
Sur	10	70	0.75		0.011	Hampton et al. (1996)
Santa Barbara	0.02	2.3	0.12		0.052	Hampton et al. (1996)
Alika-2[b]	300	95	4.8		0.051	Hampton et al. (1996)
Nuuanu[b]	5000	230	5		0.022	Hampton et al. (1996)
Tristan de Cunha[b]	150	50	3.75		0.075	Hampton et al. (1996)
Kitimat slide	0.2	6	0.2		0.033	Lipman et al. (1988)
A1	250	370	1.7		0.005	Lipman et al. (1988)
A2	22	160	1.5		0.009	Lipman et al. (1988)
A3	8.5	140	1.4		0.010	Lipman et al. (1988)
A4A	27	130	1.3		0.010	Lipman et al. (1988)
A4B	320	400	2		0.005	Lipman et al. (1988)
Kae Lae slide[b]	40	60	5		0.083	Lipman et al. (1988)
Molokai slide[b]	1100	130	5.2		0.040	Lipman et al. (1988)
Oahu slide[b]	1800	180	5.5		0.031	Lipman et al. (1988)
Alika slide[b]	1800	105	5.3		0.050	Lipman et al. (1988)
Martian landslides						
Unnamed	17880	119	7	4716	0.059	McEwen (1989)
Unnamed		56	2.4		0.043	McEwen (1989)
Unnamed	4880	70	7	1175	0.100	McEwen (1989)
Unnamed	4183	82	8.4	1244	0.102	McEwen (1989)
Unnamed	4047	94	6.8	2200	0.072	McEwen (1989)
Unnamed		52	4.4		0.085	McEwen (1989)
Unnamed	3267	76	7.2	1287	0.095	McEwen (1989)
Unnamed	2960	64	8	1675	0.125	McEwen (1989)
Unnamed	2761	63	6.8	1144	0.108	McEwen (1989)
Unnamed		50	5.4		0.108	McEwen (1989)
Unnamed	1282	63	8.2	1244	0.130	McEwen (1989)
Unnamed	833	56	5.4	1075	0.096	McEwen (1989)
Unnamed	688	45	3.6	888	0.080	McEwen (1989)
Unnamed	668	31	4.4	656	0.142	McEwen (1989)
Unnamed	655	54	7.6	470	0.141	McEwen (1989)
Unnamed	321	36	5.4	312	0.150	McEwen (1989)
Unnamed	157	33	2.8	325	0.085	McEwen (1989)
Unnamed	32	29	3.6	125	0.124	McEwen (1989)
Unnamed	29	20	4	350	0.200	McEwen (1989)
Unnamed	98[c]	18	2	175	0.111	McEwen (1989)

Table 2 (*continued*)

	V (km^3)	L_{max} (km)	H_{max} (km)	A (km^2)	H_{max}/L_{max}	References
Martian landslides						
Unnamed	11	8	1.2	44	0.150	McEwen (1989)
Unnamed	38.5[c]	21	6.4	84	0.305	McEwen (1989)
Unnamed	37.1[c]	20	6.2	81	0.310	McEwen (1989)
Unnamed	30.1[c]	19	6.2	66	0.326	McEwen (1989)
Unnamed	23.1[c]	16	5	50	0.313	McEwen (1989)
Unnamed	9.8[c]	17	6.2	22	0.365	McEwen (1989)
Unnamed	6.3[c]	7	2.2	13	0.314	McEwen (1989)
Unnamed	2.1[c]	6	2.2	4	0.367	McEwen (1989)
Unnamed	0.7[c]	8	4.2	3	0.560	McEwen (1989)
Debris flows						
Osceola	3.8			550		Iverson et al. (1998)
Tetelzingo	1.8			140		Iverson et al. (1998)
Electron	0.25			60		Iverson et al. (1998)
Round Pass	0.2			50		Iverson et al. (1998)
Dead Man Flat	0.18			90		Iverson et al. (1998)
National	0.15			78		Iverson et al. (1998)
Paradise	0.1			34		Iverson et al. (1998)
Zigzag	0.073			55		Iverson et al. (1998)
Trout Lake	0.066			27		Iverson et al. (1998)
Middle Fork Nooksack	0.05			20		Iverson et al. (1998)
Kautz Creek	0.04			4.5		Iverson et al. (1998)
Azufrado	0.04			34		Iverson et al. (1998)
Molinos Nereidas	0.03			6		Iverson et al. (1998)
Guali	0.016			11		Iverson et al. (1998)
Salt Creek	0.015			16		Iverson et al. (1998)
Tahoma	0.015			6		Iverson et al. (1998)
Oine Creek + Muddy River	0.014			18		Iverson et al. (1998)
South Fork Toutle	0.012			30		Iverson et al. (1998)
Whitney Creek	0.004			8		Iverson et al. (1998)
Bolum Creek	0.0015			3		Iverson et al. (1998)
Mabinit Eruption Lahars	0.0012			1.8		Iverson et al. (1998)
Tahoma Creek	0.0006			1		Iverson et al. (1998)
Blue Lake	0.00038			0.75		Iverson et al. (1998)
Butte Canyon	0.00038			0.5		Iverson et al. (1998)
Mabinit Typhoon Saling	0.0003			0.2		Iverson et al. (1998)
Middle Fork Nooksack	0.00014			0.4		Iverson et al. (1998)
Polallie Creek	0.00008			0.47		Iverson et al. (1998)
West Dodson	0.00008			0.1		Iverson et al. (1998)
Mayflower Gulch	0.000017			0.016		Iverson et al. (1998)
B1	0.0000003			0.002		Iverson et al. (1998)
N32	0.0000001			0.0006		Iverson et al. (1998)
N2	0.00000001			0.0002		Iverson et al. (1998)
USGS flume experiments	0.00000001			0.00025		Iverson et al. (1998)
Chillos Valley Lahar	3.8	326				Mothes et al. (1998)
Osceola	1	120				Iverson (1997)
Huascaran	0.1	120				Iverson (1997)
South Fork Toutle	0.01	44				Iverson (1997)
Muddy River	0.01	31				Iverson (1997)
Wrightwood	0.001	24				Iverson (1997)
Three Sisters	0.001	6				Iverson (1997)

(continued on next page)

Table 2 (*continued*)

	V (km^3)	L_{max} (km)	H_{max} (km)	A (km^2)	H_{max}/L_{max}	References
Debris flows						
Mount Thomas	0.0001	3.5				Iverson (1997)
Guali	0.016	103				Pierson et al. (1990)
Molinos Nereidas	0.03	69				Pierson et al. (1990)
Azufrado	0.04	69				Pierson et al. (1990)
Lagunillas	0.004	56				Pierson et al. (1990)

[a] Area estimate from Siebert (1984).
[b] Volcanic submarine landslide.
[c] The volumes estimated by extrapolation from the distal thickness by McEwen (1989) have been multiplied by 7 here. This correction was introduced after checking that, for other Martian landslides for which the volume has been estimated from the scar, the extrapolation from the distal thickness yields volume estimates which are on average seven times smaller, owing to the decrease in thickness with distance from source.

ratio as an indicator of landslide mobility implies that the energy released during the initial fall is dissipated with a constant coefficient of friction and is responsible for the runout distance. As discussed in a later section, models which use a constant coefficient of friction predict landslide velocities much higher than the velocities inferred from the control of their path by topography (Voight et al., 1983; McEwen and Malin, 1989; Voight and Sousa, 1994). The relatively low velocities inferred for natural landslides show that they rapidly dissipate the kinetic energy gained during the initial fall and so "forget" the initial fall height.

If runout essentially depends on volume and not on drop height, why do we observe a positive correlation between H_{max} and L_{max}, and a negative correlation between H_{max}/L_{max} and V? The answer may lie in the fact that landslides are forced to travel downslope on the existing topography, so H_{max} and L_{max} are not independent variables. The slope generally decreases away from the source region. If runout primarily depends on volume, the decrease in apparent friction coefficient with volume can be explained by the gentle slopes on which landslides come to rest. On such slopes, a large increase in L_{max} corresponds to a modest increase in H_{max}, thus to a decrease in H_{max}/L_{max}. The strong positive correlation between H_{max} and L_{max} (Fig. 3c) is traditionally explained by the dependence of L_{max} on H_{max}, through the apparent coefficient of friction. If we believe that L_{max} does not strongly depends on H_{max} but depends essentially on the volume, this correlation can be explained by the fact that H_{max} increases with L_{max}, as landslides travel downslope. An additional explanation is that landslides of great volume can hardly be produced from small scarps, so there must be a positive correlation between H_{max} and V (Fig. 3d) which, together with the positive correlation between L_{max} and V, produces a positive correlation between L_{max} and H_{max}.

2.4. Submarine landslides

In order to gain more insight into the factors that may enhance landslide mobility, it is interesting to compare the relationships between H_{max}, L_{max} and V for landslides occurring in different environments. The graph of H_{max}/L_{max} versus V shows the strikingly different behaviour of submarine landslides, which have much lower H_{max}/L_{max} than all other landslides, with values as low as 0.004 (Fig. 3a). An intuitive explanation would be that submarine landslides are much more mobile, as a consequence of their mixing with large amounts of water. However, when L_{max} is plotted against V, submarine landslides follow exactly the same trend as subaerial ones (Fig. 3b; Table 3). This could be interpreted as due to the compensating effects of higher mobility of the watery debris and gentler submarine slopes. Alternatively, if we follow the rationale that L_{max} is essentially a function of V and that H_{max} has only a minor influence, the similarity between the L_{max} versus V relationships of subaerial and submarine landslides could reveal similar emplacement mechanisms, despite the different environments.

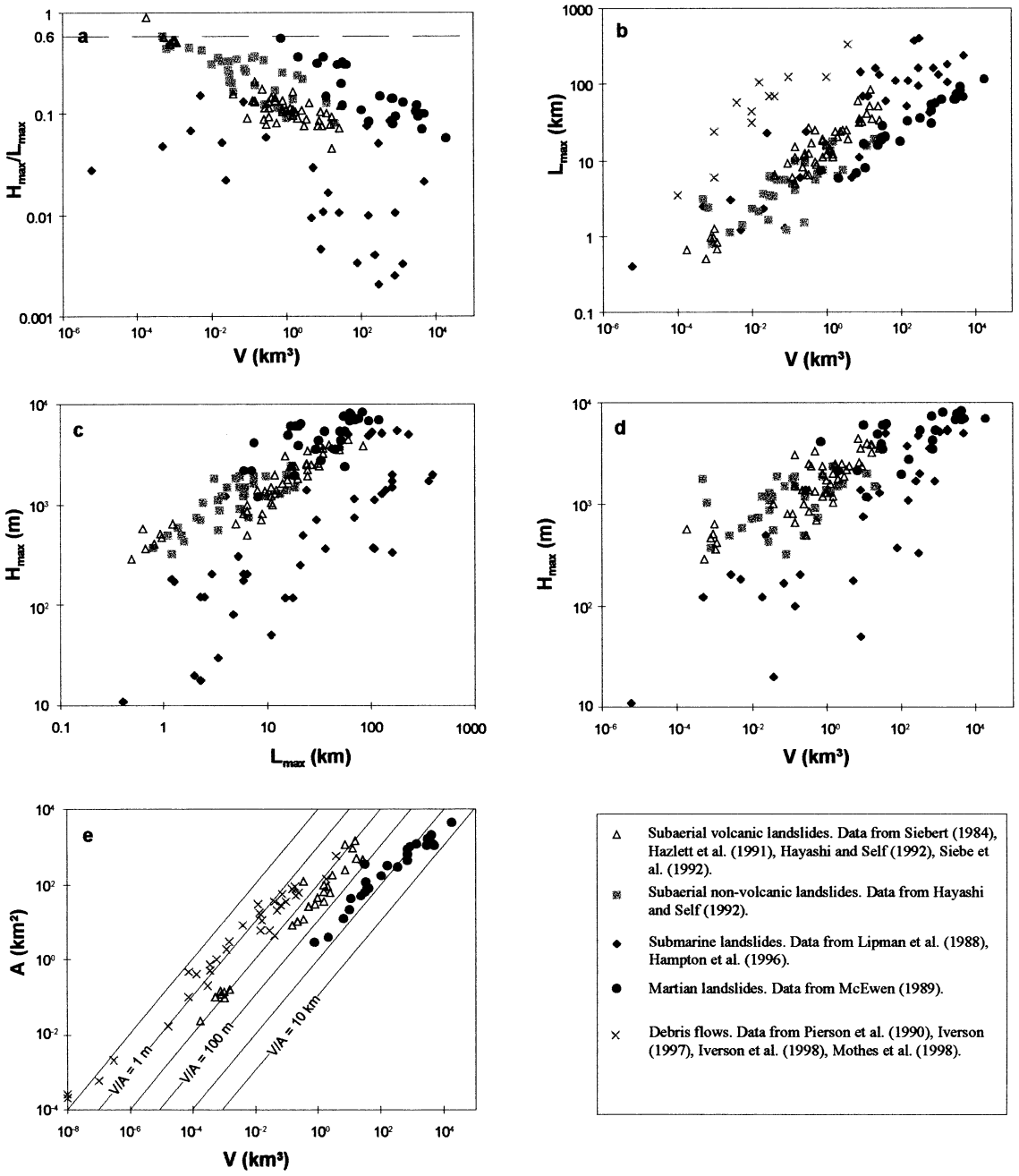

Fig. 3. Relationships between total fall height (H_{max}), runout distance (L_{max}), volume (V) and area covered by the deposit (A) for subaerial volcanic landslides, subaerial non-volcanic landslides, submarine landslides, Martian landslides and debris flows. Some deposits do not have an available estimate for one or more of these parameters, so each graph is based on a different set of data. Data are presented in Table 2. Equations of the best power-law fit to each set of data are presented in Table 3 together with the coefficients of correlation R^2. Lines in (e) indicate average deposit thickness, V/A.

Table 3
Equations of the best power-law fits of data from Fig. 3, and their coefficients of correlation R^2

	Best power-law fit	R^2
Graph of H_{max}/L_{max} versus V (Fig. 3a)		
Non-volcanic landslides	$H_{max}/L_{max}=0.16V^{-0.15}$	0.63
Volcanic landslides	$H_{max}/L_{max}=0.11V^{-0.19}$	0.81
Martian landslides	$H_{max}/L_{max}=0.42V^{-0.19}$	0.73
Submarine landslides	$H_{max}/L_{max}=0.03V^{-0.09}$	0.17
Debris flows	–	–
Graph of L_{max} versus V (Fig. 3b)		
Non-volcanic landslides	$L_{max}=8V^{0.25}$	0.6
Volcanic landslides	$L_{max}=15.6V^{0.39}$	0.91
Martian landslides	$L_{max}=6.2V^{0.34}$	0.92
Submarine landslides	$L_{max}=18V^{0.33}$	0.79
Debris flows	$L_{max}=235V^{0.39}$	0.82
Graph of H_{max} versus L_{max} (Fig. 3c)		
Non-volcanic landslides	$H_{max}=486L_{max}^{0.52}$	0.66
Volcanic landslides	$H_{max}=412L_{max}^{0.53}$	0.85
Martian landslides	$H_{max}=1200L_{max}^{0.38}$	0.42
Submarine landslides	$H_{max}=47L_{max}^{0.73}$	0.63
Debris flows	–	–
Graph of H_{max} versus V (Fig. 3d)		
Non-volcanic landslides	$H_{max}=1310V^{0.09}$	0.2
Volcanic landslides	$H_{max}=1780V^{0.20}$	0.72
Martian landslides	$H_{max}=2660V^{0.11}$	0.36
Submarine landslides	$H_{max}=387V^{0.29}$	0.7
Debris flows	–	–
Graph of A versus V (Fig. 3e)		
Non-volcanic landslides	–	–
Volcanic landslides	$A=55V^{0.87}$	0.97
Martian landslides	$A=6.1V^{0.70}$	0.93
Submarine landslides	–	–
Debris flows	$A=230V^{0.76}$	0.97

Note the generally better R^2 for the graph of L_{max} versus V compared with the graph of H_{max}/L_{max} versus V, and the relatively constant value of the exponent ($\sim 1/3$) in the relation between L_{max} and V for the various types of deposits.

In submarine settings, velocity is partly controlled by the turbulent drag exerted by seawater on landslide surface. As turbulent drag scales with the square of the velocity, any high velocity initially acquired down a steep slope is rapidly lost (Norem et al., 1990). On the other hand, the extent to which water is incorporated to the moving submarine landslide and increases its mobility is unknown. In subaerial settings, it is widely accepted that a landslide in which the water content becomes sufficiently high can transform into a debris flow (e.g., Iverson, 1997), and there are well-documented examples of such transformations, as at Huascarán (Plafker and Ericksen, 1978), Mount St. Helens (Voight et al., 1983), Mount Rainier (Vallance and Scott, 1997), Cotopaxi (Mothes et al., 1998) or Ontake-san volcano (Takarada et al., 1999). Morphologically, debris-flow deposits are distinguished by their longer runout, smaller thickness and smoother surface, generally lacking the hummocks typical of landslide deposits, although deposits with intermediate characteristics are found within this continuum. One would therefore expect that, in submarine settings, landslides rapidly transform into debris flows. Surprisingly, this does not always occur, and many submarine landslide deposits have a morphology more typical of subaerial landslides than of debris flows (Lipman et al., 1988; Moore et al., 1994). Their runout (or area) versus volume relationship also shows that they are less mobile than debris flows and as mobile as subaerial landslides (Fig. 3b; Table 3). These features may suggest that submarine landslides, like subaerial ones, are not fully saturated with water.

For submarine landslides which originate subaerially, the rate of percolation of seawater into the landslide body (q) can be evaluated through the law of Darcy,

$$q = \frac{k}{\eta}\frac{\mathrm{d}P}{\mathrm{d}x}, \tag{1}$$

where k is the permeability of the debris, η is the viscosity of water, and $\mathrm{d}P/\mathrm{d}x$ is the gradient of total mechanical potential of fluid. If the initial pore pressure within the landslide is assumed negligible with respect to hydrostatic pressure, $\mathrm{d}P$ is simply the pressure of the seawater column at the surface of the landslide and $\mathrm{d}x$ is the distance to which water has already penetrated the debris. Permeability of the poorly sorted material involved in landslides and debris flows can vary between 10^{-9} and 10^{-13} m^2 (Voight et al., 1983; Iverson, 1997). In this problem, it seems reasonable to choose values at the lower end of the range as the material would be compressed below water. By using $k=10^{-13}$ m^2 and a pressure of 4000 m of water, the maximum depth where submarine landslides deposits are known, we obtain a percolation rate of only 4 mm s^{-1} once water has penetrated the first metre of debris,

and this rate would rapidly decrease as water penetrates deeper into the debris. This estimates would still be lower if the viscosity of a slurry composed of water plus the finest particles in the debris was used in Eq. (1) instead of the viscosity of clear water. Given typical emplacement times on the order of 1000 s, it seems possible that some large landslides which enter the sea remain unsaturated with water.

Landslides which originate below water must be initially saturated. However, the dilation which accompanies the initiation of some landslides would create a significant pore volume free of water. Alternatively, if submarine landslides are really saturated with water, there must be an unknown mechanism which prevents them from transforming into debris flows.

In any case, the morphological similarities between subaerial and submarine landslide deposits, and their differences with subaerial and submarine debris-flow deposits raise the possibility that submarine landslides have essentially the same dynamics as their subaerial counterparts. In that case, the similar relation between L_{max} and V may simply reflect this fact. The much lower H_{max}/L_{max} ratios for submarine landslides would reflect the gentler slopes on which submarine landslides can be triggered (Hampton et al., 1996).

2.5. Martian landslides

The behaviour of Martian landslides also shows some difference with respect to terrestrial ones. In the graph of H_{max}/L_{max} versus V, Martian landslides have a higher apparent friction coefficient than terrestrial landslides of the same volume (Fig. 3a). If runout does not depend strongly on drop height, this could be partly explained by the very high scarps from which most Martian landslides initiate. Nevertheless, in the graph of L_{max} versus V, Martian landslides still have runouts nearly two times shorter than terrestrial ones for a given volume (Fig. 3b).

McEwen (1989) proposed that the lower mobility of Martian landslides could be explained if landslide runout was controlled by the yield strength of the material. A viscoplastic material which possesses a yield strength spreads on an incline until its thickness becomes less than a threshold value (h_c) which depends on its bulk density (ρ_b), its yield strength (Y), the slope angle (β) and the gravity acceleration (g) (Johnson, 1970; Battaglia, 1993),

$$h_c = \frac{Y}{\rho_b g \sin\beta}. \quad (2)$$

For a given yield strength, landslides on a planet with a greater gravity (the Earth) would spread to a smaller thickness, and thus would have a longer runout. There are however at least two problems with this analysis. First, Eq. (2) neglects landslide inertia and, second, it predicts that the thickness of the deposit should not depend on its volume. The latter is in contradiction with data from both terrestrial and Martian landslides, which show a positive correlation between average thickness and volume (Fig. 3e). Landslides deposits cover areas approximately proportional to $V^{2/3}$ (Hungr, 1990a; Dade and Huppert, 1998), which means that their average thickness is roughly proportional to $V^{1/3}$. If thickness was controlled by yield strength, the positive correlation between thickness and volume would imply that more voluminous landslides have a greater strength, for which there is no apparent reason. Moreover, the thickness of the deposit should be less where the slope is steeper. In contrast, landslide deposits are generally thicker near source, where slope is steeper. Therefore, thickness data from landslide deposits are not consistent with their formation by en masse freezing due to a yield strength. This does not rule out that landslides may indeed possess a yield strength and that their upper part may stop en masse, as suggested by the morphology of their deposits, but sudden freezing of the whole mass when it reaches a critical thickness seems unlikely.

An alternative reason for the lower mobility of Martian landslides is that they probably contain less water than most terrestrial landslides. The role of fluids has often been invoked to explain landslide mobility and will be examined in more details in a later section.

3. Landslides as granular flows

The importance of fluids for landslide mobility has been questioned after the discovery of large landslide deposits on the Moon and on Mars (Howard, 1973;

McEwen, 1989). This has led some authors to explore the possibility that landslides travel as granular flows, without the need of any interstitial fluid (Melosh, 1979; Davies, 1982; Campbell, 1989; Cleary and Campbell, 1993; Campbell et al., 1995; Straub, 1996, 1997). Following the pioneering work by Bagnold (1954), the mechanics of granular flows has become an important area of research. However, despite significant advances, the understanding of granular flows is still too rudimentary to allow a rigorous application to geological flows. One major limitation of current theories is that they are not yet able to model flows with a wide range of particle sizes, like those occurring in nature. Even for more simple cases, with only one particle size, there are still discrepancies between some theoretical and experimental results. For example, numerical simulations of rapid granular flow that use periodic boundaries show an expanded shearing basal layer below a non-expanded, non-shearing plug (Cleary and Campbell, 1993; Straub, 1996, 1997), a flow structure similar to that hypothesised for landslides by some authors (Davies, 1982; Campbell, 1989). In contrast, laboratory experiments (Drake, 1990) and numerical simulations of a finite granular mass released on an incline (Campbell et al., 1995) do not show such an expanded shearing basal layer and have an upward-decreasing density.

The granular flow theory distinguishes two regimes, frictional and collisional. In the frictional, quasistatic regime, grains move slowly and dissipate energy through long-lasting, frictional contacts. The dissipative stress is the product of the coefficient of friction and the normal stress due to the overburden. In the collisional, rapid flow regime, grains are more agitated and dissipate energy through short-lived collisional contacts. The dissipative shear stress (τ_s) is proportional to the square of the vertical velocity gradient (dU/dy) and to a positive function of the particle concentration (f)

$$\tau_s = f\sigma D^2 \sin\alpha \left(\frac{dU}{dy}\right)^2, \quad (3)$$

where α is the critical dynamic angle of internal friction, σ is the density of particles and D their diameter (Bagnold, 1954; Savage and Hutter, 1989; Campbell, 1990). From Eq. (3), one would anticipate that, in this regime, the dissipative stress will increase with flow velocity. In contrast, experiments give the surprising result that the dissipative stress does not vary, or only little, with velocity (Hungr and Morgenstern, 1984a,b; Hanes and Inman, 1985; Savage and Hutter, 1989). This can be explained by the fact that particle collisions also generate a dispersive normal stress or dispersive pressure (P_d), which Bagnold (1954) showed to be proportional to the shear stress

$$P_d = \frac{\tau_s}{\tan\alpha}. \quad (4)$$

In a fully developed collisional flow, dispersive normal stress must be able to support the whole load of the overburden and so is equal to static pressure. When flow velocity increases, dispersive normal stress should increase too. But as soon as it becomes higher than the overburden load, the flow immediately expands, particle concentration decreases and consequently the dispersive normal stress decreases, until it is again just able to support the overburden. By this mechanism, in the collisional regime, the dispersive normal stress is always forced to be equal to the static pressure of the overburden, and so the shear stress, which is proportional to the dispersive normal stress, is also forced to be constant,

$$\tau_s = \mu N, \quad (5)$$

where N is the normal static pressure of the overburden and μ is the coefficient of friction, $\mu = \tan\alpha$. The Coulomb condition of constant coefficient of friction, valid in the frictional regime, therefore also holds in the rapid, collisional regime (Hungr and Morgenstern, 1984a,b; Hanes and Inman, 1985; Savage and Hutter, 1989; Straub, 1996, 1997), which means that a rapid, collisional granular flow cannot travel further than a frictional flow.

We may however wonder whether a landslide that would progressively lose mass due to deposition could not maintain a higher velocity and travel further than a landslide that would move and stop as a single block. Several authors have proposed models in which runout was modified owing to progressive mass change during transport (Cannon and Savage, 1988;

Van Gassen and Cruden, 1989; Voight and Sousa, 1994). Using a model based on the principle of conservation of momentum, Van Gassen and Cruden (1989) suggested that even the distance travelled by the centre of mass would increase for a landslide that would lose mass during transport. An analysis by Cannon and Savage (1988) based on the same principle was however criticised because it ignores the work necessary for the mass change (Hungr, 1990b; Erlichson, 1991). When a flow entrains an immobile mass and accelerates it up to its own velocity, momentum is conserved but the total kinetic energy of the system decreases because the entrainment and acceleration process is equivalent to an inelastic collision in which all the collisional energy is lost. In contrast, when a flow loses mass, using the conservation of momentum equation would imply an increase in the total kinetic energy of the system. This is clearly illustrated by the fact that, in the model of Van Gassen and Cruden (1989), the centre of mass is able to travel further than predicted by energy conservation arguments, which implies that there is more frictional work done by the landslide than potential energy lost. Conservation of momentum is correctly used to describe the motion of a rocket because the rocket engine does provide energy (Hungr, 1990b; Erlichson, 1991). In a landslide, however, there is no source of energy other than that derived from the loss of potential energy, so the conservation of momentum equation cannot be used. It follows that, even if mass is progressively lost, the centre of mass cannot travel further than in a constant-mass model.

Now, this does not mean that the *runout* (L_{max}) of frictional and collisional flows cannot be increased owing to progressive mass loss. This is illustrated by the following simple example. Consider two blocks of same mass sliding along a topography such as that represented in Fig. 4. If the blocks stick together and move as a single block, they travel until the centre of mass reaches a distance L for which H/L is equal to the coefficient of friction (Fig. 4a). If the blocks move separately, the centre of mass of the first block reaches the same distance L (Fig. 4b). The second block would like to do the same, but before it arrives at distance L, it collides with the first block (Fig. 4c). If collision is elastic, the second block stops (it "deposits") and transmits all its kinetic energy to the first block which can thus travel an excess distance (Fig. 4d). Comparison between Fig. 4a and d shows that runout (L_{max}) for the changing-mass slide is longer than for the constant-mass slide, although the distance travelled by the centre of mass (L) is the same. For a landslide containing a great number of particles, this mechanism of spreading by deposition would produce a continuous deposit. Note that in the block-sliding example described above, we assume that collision is elastic because energy is already dissipated through basal friction and an inelastic collision would cause an extra loss of energy. In a fully developed collisional granular flow, particle collisions are inelastic but this does not imply extra loss of energy as, in this regime, frictional stress is negligible and inelastic collisions are the only way by which energy is dissipated.

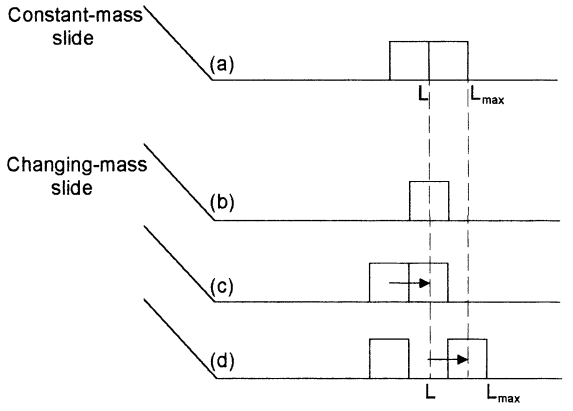

Fig. 4. Schematic comparison between a constant-mass slide (a) and a changing-mass slide (b–d). (a) The two blocks stick together and slide as a single block. (b) Block 1 slides first and reaches L. (c) Block 2 collides with block 1, stops and transmits its kinetic energy. (d) Block 1 slides an excess distance. L = distance travelled by the centre of mass; L_{max} = maximum distance travelled.

The excess runout due to mass deposition depends on the rate of mass change. Cannon and Savage (1988) and Van Gassen and Cruden (1989) investigated the effect of arbitrarily imposed mass-change rates on runout. Here, a model is proposed in which the mass-change rate is a consequence of the deceleration of a rapid granular flow and not an independent variable. We consider a granular flow initially in the collisional regime which decelerates on a gentle slope. As velocity decreases, dispersive normal stress decreases. As soon as it becomes less than the load of the overburden, the base of the flow immediately

compacts and particle concentration increases, until the normal stress is again equal to the load of the overburden. However, particle concentration cannot increase indefinitely, and when it approaches a certain threshold value, frictional stress becomes dominant over dispersive stress. Only above a certain level can the flow still move in the collisional regime, while the basal portion is now in the frictional regime. As velocity continues decreasing, the boundary between the frictional base and the collisional upper portion of the flow moves upward. This behaviour is shown in numerical simulations of decelerating rapid granular flows (Straub, 1997). As one would expect, the frictional base is much slower than the collisional top. Straub (1997) indicates that the part in the frictional regime does not contribute significantly to the flow motion and that, in practice, the passage from the rapid, collisional regime to the quasistatic, frictional regime may be viewed as deposition. A similar process is also shown in the experiments by Hanes and Inman (1985), in which a granular material is sheared in an annular cell. Only the upper portion of the granular material moves in the rapid collisional regime, while the lower portion is frictionally locked to the bottom of the annular cell. When the imposed shear stress is progressively lowered, the thickness of the granular material moving in the collisional regime decreases, which means that the interface between the rapid, collisional and quasistatic, frictional regions progressively shifts upward (Hanes and Inman, 1985). The deposit at the base of a slowing granular flow may therefore form by upward, progressive accretion.

We can now test whether the mass lost in this manner can account for a significant increase in runout. As deduced from Eqs. (3) and (4), the dispersive normal stress is given by

$$P_{\mathrm{d}} = f\sigma D^2 \cos\alpha \left(\frac{\mathrm{d}U}{\mathrm{d}y}\right)^2, \tag{6}$$

while the normal static stress due to the overburden is

$$N = \rho_{\mathrm{b}} g h \cos\beta, \tag{7}$$

where ρ_{b} is the bulk density of the landslide, h is its depth and β is the slope. Consider a landslide of mass m in the collisional regime debouching in a valley of negligible slope ($\beta \sim 0$), with a mean velocity U. As the shear stress is described by Eq. (5), the variation of kinetic energy with distance will be described by

$$\frac{\mathrm{d}E}{\mathrm{d}x} = \frac{U^2}{2}\frac{\mathrm{d}m}{\mathrm{d}x} + mU\frac{\mathrm{d}U}{\mathrm{d}x} = -\mu g m. \tag{8}$$

Note that this approach is different from that which considers conservation of momentum. Here, we consider that energy, not momentum, is conserved, for the reasons outlined above. As the slope is less than the angle of friction ($\tan\beta < \mu$), the landslide decelerates. The decrease in velocity can first be compensated by an increase in granular concentration at the base of the flow but, beyond a certain concentration (f_{c}), particle interactions become dominantly frictional. The dispersive normal stress can no longer support the load of the whole landslide and only the upper part can proceed in the rapid granular flow regime while the base slows down and deposits. By equating the static normal stress (Eq. (7)) with the dispersive normal stress (Eq. (6)), the thickness of the upper part of the landslide which still moves in the rapid flow regime is found to be

$$h = \frac{f_{\mathrm{c}}\sigma D^2 \cos\alpha}{\rho_{\mathrm{b}} g}\left(\frac{\mathrm{d}U}{\mathrm{d}y}\right)^2. \tag{9}$$

Eq. (9) can be simplified by assuming that $\mathrm{d}U/\mathrm{d}y = U/h_{\mathrm{s}}$, where h_{s} is the typical thickness over which shearing occurs. It is not very clear whether h_{s} should scale with the grain diameter (e.g., Cleary and Campbell, 1993; Straub, 1996) or with the flow thickness (e.g., Drake, 1990; Campbell et al., 1995; Mills et al., 1999). We first consider the case in which h_{s} is equal to a few times the typical grain diameter and so is independent of h, then the case in which h_{s} is proportional to h. In the first case, we have that

$$h = \frac{f_{\mathrm{c}}\sigma D^2 \cos\alpha U^2}{\rho_{\mathrm{b}} g h_{\mathrm{s}}^2} = B_1 U^2, \tag{10}$$

where

$$B_1 \equiv \frac{f_{\mathrm{c}}\sigma D^2 \cos\alpha}{\rho_{\mathrm{b}} g h_{\mathrm{s}}^2}. \tag{11}$$

As shown by Eq. (8), before the landslide starts depositing, the loss of kinetic energy due to granular stress is entirely accommodated by a decrease in the

mean velocity. When deposition starts, the loss of kinetic energy is accommodated by both a decrease in the mean velocity and a loss of mass of the moving landslide. The mass of the moving landslide can be expressed by $m = \rho_b A h$. Assuming that the area (A) of the moving landslide does not vary with time, we can transform the energy equation, Eq. (8), into

$$\frac{U^2}{2h}\frac{dh}{dx} + U\frac{dU}{dx} = -\mu g \tag{12}$$

and upon substituting h by $B_1 U^2$ (Eq. (10)), we see that

$$\frac{dU}{dx} = -\frac{\mu g}{2U}. \tag{13}$$

This shows that, due to deposition, the deceleration of the moving landslide is two times less than in a non-depositing case. The runout distance is obtained by integrating Eq. (13) up to the distance L_{max} at which U becomes zero, which yields

$$L_{max} - x_0 = \frac{U_0^2}{\mu g}, \tag{14}$$

where x_0 is the distance where deposition starts, at which $U = U_0$. Eq. (14) shows that using a friction coefficient of 0.5 and a velocity of 100 m s^{-1} at the beginning of deposition would allow spreading of the landslide over only 2 km. Unrealistically high velocities or low friction coefficients should be assumed if the much larger distances over which natural landslides spread and deposit are to be explained by this model.

We can also calculate the distance travelled by the centre of mass (L). By substituting Eq. (10) into Eq. (12), we get the following expression for the loss of mass from the moving landslide by unit distance

$$\frac{dh}{dx} = -B_1 \mu g. \tag{15}$$

As the thickness of the deposit left at a given distance must be proportional to $-dh/dx$, Eq. (15) predicts that thickness will be constant over the whole length of the deposit. Therefore, the centre of mass will be at a distance

$$L = x_0 + \frac{(L_{max} - x_0)}{2}. \tag{16}$$

By substituting Eq. (14) into Eq. (16) and by giving its value to the initial velocity U_0,

$$U_0 = (2g(H - \mu x_0))^{\frac{1}{2}}, \tag{17}$$

one finds that L is simply equal to H/μ, where H is the drop height of the centre of mass. As expected, the distance travelled by the centre of mass has not been increased by the mass change because no energy other than that derived from the loss of potential energy has been supplied to the landslide.

If we consider now the case where the typical thickness of shearing, h_s, is equal to the depth of the moving landslide, h, Eq. (10) becomes

$$h = B_2 U^{\frac{2}{3}}, \tag{18}$$

with B_2 defined as

$$B_2 \equiv \left(\frac{f_c \sigma D^2 \cos\alpha}{\rho_b g}\right)^{\frac{1}{3}}. \tag{19}$$

Substituting into Eq. (12) gives

$$\frac{dU}{dx} = -\frac{3}{4}\frac{\mu g}{U}. \tag{20}$$

Deceleration is stronger than for the first case (Eq. (13)) and so L_{max} is shorter. L remains equal to H/μ.

It is important to stress that the rate of mass loss and the runout increase calculated here are based on several simplifications and, in particular, on the assumptions that the granular flow is initially in the collisional regime and that the growing, friction-dominated basal portion has negligible velocity. Unfortunately, it is difficult to evaluate whether natural landslides can indeed be in the collisional regime, because the way interparticle collisions dissipate energy in a poorly sorted debris is still poorly understood. Notwithstanding this, the most important conclusion of this analysis of a changing-mass granular flow is that, as long as the Coulomb condition of constant coefficient of friction holds, progressive deposition does not allow the centre of mass to travel further than the distance expected for a sliding block, neither in the frictional nor in the collisional regime. This conclusion is a direct consequence of using the principle of conservation of energy; it does not depend on the specific simplifications and assumptions made here and is not modified if we consider a slope $\beta > 0$. Therefore, in order to explain the long runout of

landslides by granular spreading, we have to assume either that the Coulomb condition of a constant coefficient of friction does not hold, or that the effective coefficient of friction is smaller than the normal value of μ for rocks.

The possibility that the Coulomb condition of constant coefficient of friction may break down in large granular landslides has been suggested by Campbell et al. (1995). Their numerical simulations of granular, fluid-absent landslides show apparent coefficients of friction as low as those of natural landslide deposits, and also reproduce the negative correlation observed in nature between volume and apparent coefficient of friction. The numerical landslides of Campbell et al. (1995) travel in a regime intermediate between frictional and collisional and the authors speculate that this might be the reason for the breakdown of the Coulomb condition, although they recognise that there is currently no theoretical explanation nor experimental evidence for this. The simulations are presented as non-dimensional, as the volume, drop height, runout and velocity are non-dimensionalised by the particle diameter. It follows that the apparent coefficient of friction in these simulations actually depends on the *number* of particles, not on the volume of the landslide. For example, Fig. 12 of Campbell et al. (1995) shows that the decrease in apparent coefficient of friction with increasing volume observed in natural landslides is correctly reproduced in the simulations only if the particle diameter is 1 m (Fig. 5). It can be seen that, if the diameter is taken to be 0.1 or 10 m, the numerical results plot well outside of the field of natural data. If the simulations are truly non-dimensional, the same negative correlation between volume and apparent coefficient of friction should occur at smaller volumes for smaller particles. As shown in Fig. 5, apparent coefficients of friction as low as 0.1 should occur for volumes of 1 m^3 and particle diameters of 1 mm, or volumes of 1 dm^3 and particle diameters of 0.1 mm. It is interesting to note that, in laboratory experiments that use volumes between 0.1 dm^3 and 1 m^3 and grainsizes of 0.2 and 2 mm, apparent coefficients of friction measured from the runout distance L_{max} can be much lower than the actual coefficient of friction of the material (Davies and McSaveney, 1999). However, the most surprising result of the numerical simulations of Campbell et al. is that the apparent coefficient of friction measured from *the centre of mass* is also negatively correlated with volume. In

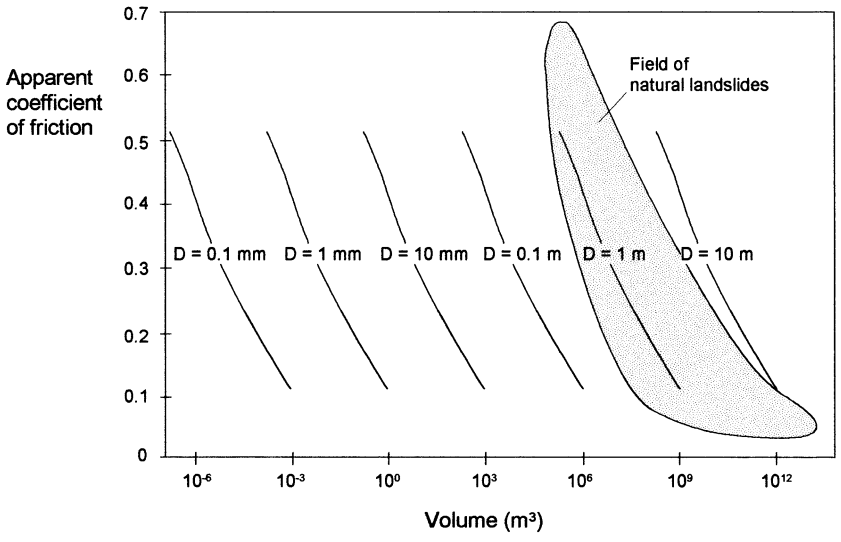

Fig. 5. Correlation between apparent coefficient of friction and landslide volume predicted by the numerical simulations of Campbell et al. (1995) for different particle diameters (*D*). For a given volume, simulations predict lower apparent coefficients of friction for higher numbers of particles, hence for smaller particle diameters.

contrast, Davies and McSaveney state that the translation of the centre of mass is similar for large- and small-scale avalanches, although they do not provide data in support of this statement.

It is difficult to evaluate the effect of the boundary roughness and particle circularity in the simulations of Campbell et al. (1995). While the numerical simulations by Cleary and Campbell (1993) had emphasised the strong influence of boundary roughness on runout, Campbell et al. do not indicate the boundary condition used. On perfectly smooth boundaries, simulations by Cleary and Campbell show that particle circularity causes a runout of small landslides much larger than expected, due to particle rolling, in contrast with what occurs in natural small landslides. One may therefore wonder whether particle rolling might not be partly responsible for the mobility of the large-landslide simulations of Campbell et al., and to which extent the results are applicable to natural landslides. A better understanding of the transitional regime and of the effect of a wide grainsize distribution in granular flows is required in order to evaluate whether the mobility of natural landslides can be explained by fluid-absent, granular models. At present, there is no firm evidence for this.

4. Role of fluids

4.1. Reduction of the solid coefficient of friction

The fact that landslides can travel larger distances than expected from simple frictional arguments has led many authors to hypothesise that fluids play a significant role in reducing solid friction (e.g., Kent, 1966; Shreve 1968a,b; Goguel 1978; Johnson, 1978; Voight et al., 1983; Voight and Sousa, 1994). Addition of an interstitial fluid can reduce the effective coefficient of solid friction of a granular material by partly supporting particles, thus reducing the normal granular stress (Bagnold, 1954). The upward force exerted upon a particle immersed in a fluid is equal to the product of the fluid pressure gradient and the particle volume. In the simple case where the fluid pressure gradient is hydrostatic, the normal granular stress is

$$N = g(\sigma - \rho_f)Ch, \tag{21}$$

where ρ_f is the density of the interstitial fluid, C is the particle concentration and the slope is again assumed negligible ($\beta \sim 0$) to be consistent with the equations derived above. As granular shear stress is related to normal stress by $\tau_s = \mu N$, it can be expressed by

$$\tau_s = \mu g(\sigma - \rho_f)Ch. \tag{22}$$

The decrease in kinetic energy with distance due to granular shear stress is

$$\frac{dE}{dx} = -\mu \frac{(\sigma - \rho_f)C}{\rho_b} gm, \tag{23}$$

where ρ_b is the bulk density of the landslide defined as

$$\rho_b = \rho_f(1 - C) + \sigma C. \tag{24}$$

Compared with Eq. (8), the effective coefficient of friction in Eq. (23) has been decreased by a factor $(\sigma - \rho_f)\, C/\rho_b$. It can become very low if the density of the interstitial fluid (typically water plus fine particles) is important relative to that of large particles.

The pressure gradient in the fluid can also be in excess of hydrostatic. If it becomes equal to the lithostatic pressure gradient, the whole load of the solid material is supported by the fluid and the solid friction effectively reduces to zero. The flow is said to be liquefied, or fluidised. Iverson (1997) showed that transient pore fluid pressures exceeding hydrostatic pressures occur in experimental debris flows and act to reduce energy dissipation and enhance flow mobility.

Eq. (23) does not take into account the viscous stress due to the interstitial fluid. When solid friction becomes very low, viscous dissipation may become dominant, and the landslide behaves like a fluid, with a dissipative stress proportional to the velocity gradient. Energy dissipation may therefore become higher on steep slopes and lower on gentle slopes. We shall see in a later section that this is qualitatively consistent with the way landslides respond to topography.

4.2. Fluids in extraterrestrial landslides

The idea that fluids are important for landslide mobility was dealt a severe blow by the discovery of landslide deposits that had travelled unexpectedly

large distances on the Moon (Howard, 1973) and on Mars (Lucchitta, 1978, 1979, 1987; McEwen, 1989). The evidence that extraterrestrial landslides travelled great distances in fluid-absent conditions is however equivocal. On Mars, the atmosphere pressure is about 100 times less than on the Earth and its possible role in fluidising landslides is probably negligible. More significant is the presence of ground ice at shallow depths. Lucchitta (1978, 1979, 1987) believed that Martian landslides were emplaced as wet debris avalanches. McEwen (1989) rejected this hypothesis and proposed that they were dry. The term *dry* was clearly used to refer to *unsaturated* debris avalanches, as opposite to *wet* debris flows assumed to be saturated in water. Indeed, one argument of McEwen for the dry nature of Martian landslides was the similarity of their deposits with those of landslides on the Earth. There would be a circularity in the reasoning if we were now using the dry nature of Martian landslides to conclude that water is unimportant for the mobility of terrestrial landslides, when the dry nature of Martian landslides has been inferred from their resemblance with terrestrial ones. The other argument of McEwen (1989) against a wet emplacement of Martian landslides was that, in the region where they occurred, the ground was probably depleted of ice to depths of 100 m or more. However, as all these landslides have estimated volumes between 10^8 and 10^{13} m^3, most of them involved failure to depths probably well below 100 m, sometimes up to several kilometres. They are therefore likely to have contained a substantial volume of ground ice. At least part of the ice should rapidly melt during landslide emplacement, and liquid water would remain stable within the landslide due to the pressure of the overburden. The smallest landslide presented by McEwen (1989) has a volume of 10^8 m^3 and an H/L ratio close to 0.6, much higher than that typical of terrestrial landslides of similar volume. This is about the value expected from purely frictional arguments and it may reflect the relative dryness of this small landslide, probably constituted of superficial, ice-depleted rocks. The fact that no landslide smaller than 10^8 m^3 has been described on Mars, if it is not an artefact due to the low resolution of images or to a lower interest in small structures, might reflect the difficulty for triggering landslides in superficial, dry material.

A long-runout landslide deposit was described on the Moon, where atmosphere and water are absent (Howard, 1973). The deposit around the Tsiolkovsky impact crater has also been interpreted by some authors as the result of a large lunar landslide (Guest, 1971; Hsü, 1975). Both events are however suspected to have been triggered by impacts, which would have provided additional energy, so they may have been emplaced partly as ejecta (Howard, 1973; Lucchitta, 1977). If we put these questionable cases aside, the striking feature on the Moon is the *lack* of long-runout landslide deposits. The steep inner walls of impact craters are affected by large slumps and small granular avalanches, which do not extent further than expected from the repose angle of the material. Evidence from the Moon might therefore suggest that fluids are indeed essential for the generation of long-runout landslides.

4.3. Lubrication by a basal air layer

Shreve (1968a) proposed that the Blackhawk landslide overrode, trapped and compressed a cushion of air over which it slid with little friction. By estimating the volume of compressed air that had been trapped, Shreve (1968b) deduced that the leakage rate had to be less than 1 mm s^{-1} in order to maintain the lubricating air layer during the time of landslide emplacement. By using a sophisticated form of the Darcy equation and assuming an air-pressure gradient equal to the lithostatic gradient, he proposed that a permeability of 10^{-12} m^2 was required, a reasonable value for the very poorly sorted debris typical of landslides (Iverson, 1997).

The major problem with this analysis is that it assumes that the debris has a fixed permeability which controls the leakage rate. Experiments on fluidisation (e.g., Wilson, 1984) show that the permeability of a sediment can dramatically increase when it is fluidised. In these experiments, a controlled flux of air is passed upward through a bed of sediment resting on a permeable support. The air pressure at the base of the bed is measured with a manometer. As long as the air pressure gradient is less than lithostatic, it varies linearly with the imposed flux (or velocity) as expected from the Darcy equation (Eq. (1)). Once the air pressure gradient becomes lithostatic, it does not increase any longer with an increase of the imposed flux (Fig. 6). This is easy to

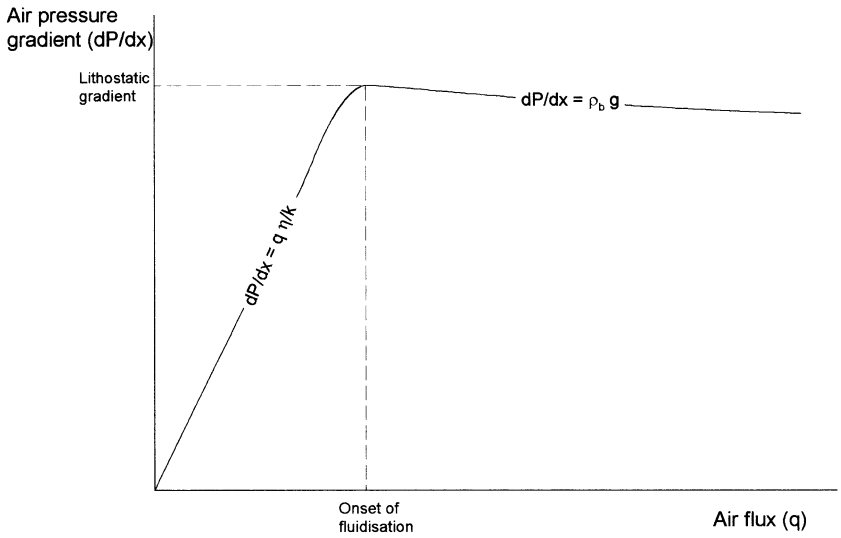

Fig. 6. The relation between air pressure gradient and air flux in fluidisation experiments. As long as the sediment bed is not fluidised, air pressure gradient increases linearly with air flux, at a rate inversely proportional to its permeability (k). When the bed is fluidised, the air flux can be increased without increasing the pressure gradient, which remains equal to the lithostatic pressure gradient ($\rho_b g$) of the bed. This implies that the effective permeability increases. The slight decrease in air pressure gradient with air flux is caused by the slight decrease in the sediment bulk density due to bed expansion.

understand as, once the air is able to support the weight of the bed, a slight expansion of the bed dramatically increases its permeability and allows a much greater flux of air to be passed. In other words, for air pressure gradients lower than lithostatic, permeability controls air flux, while, for air pressure gradients equal to lithostatic, air flux controls permeability. In practice, for gas fluidisation, effective permeability is increased with a very slight expansion of the bed, as the extra fluid is passed through the bed in the form of bubbles (Wilson, 1984).

In the air-layer lubrication model, a fixed amount of air is compressed below the landslide at lithostatic pressure. In this situation, air flux will control permeability and not the contrary, so the analysis of Shreve (1968b) which treats the landslide as a coherent, porous block of fixed permeability is flawed. What then will control the velocity of air leakage through the debris and so the time during which the air cushion can suppress basal friction? If the flux of air leaking through the debris cannot be restricted by permeability, the debris should be able to fall essentially unhindered. In fact, the situation in which a dense granular debris is entirely supported by a light gas is not stable, even if theoretically the gas pressure gradient is able to support the debris. The granular debris would fall by batches and the gas would rise as large bubbles, hence much more rapidly than if controlled by the permeability of the debris. Even in a static column, a poorly sorted granular debris can fall virtually unhindered by air. It is therefore extremely difficult to conceive how particles within an agitated landslide could remain locked together and avoid falling through the basal air layer, even pressurised.

4.4. Fluidisation by air

If the air-layer lubrication hypothesis is seriously questioned, this does not rule out that landslides might be partly *fluidised* by air. Complete fluidisation of a sediment bed occurs when the pore fluid pressure gradient in the bed is lithostatic, so that it can support the load of the overburden and, in a flow, reduce granular friction. As the bed is pervious and denser than the interstitial fluid, lithostatic pore pressure gradients provoke the upward escape of the fluid. Thus, maintaining the lithostatic pressure gradient requires a continuous supply of fluid at the bottom

of the bed. As this is unlikely in landslides, what must be evaluated is whether high pore pressures can be maintained for a time comparable to that of landslide emplacement.

If the air pressure gradient is just less than lithostatic, permeability and consequently the rate of air escape are kept low (see Fig. 6). The presence of an air pressure gradient lower than lithostatic would still act to lower the normal granular stress, hence the friction. As shown by the equation of Darcy (Eq. (1)), a debris with permeability 10^{-11} m^2 could be fluidised with a flux of air of about 1 cm s^{-1}. In the absence of a continuous supply of air at the bottom, fluidisation would require a net downward movement of the granular material (Iverson, 1997), i.e., progressive aggradation of the deposit by hindered settling (Druitt, 1995). If we can assume that the debris compacts by 10% when it deposits, a 10-cm s^{-1} aggradation rate is required to release 1 cm of air per second at the base of the moving debris. A 10-cm s^{-1} aggradation rate would leave a 10-m-thick deposit in 100 s, which is in good match with the thickness and travel time of the Blackhawk landslide (Shreve, 1968a,b). Thicker landslides would be able to travel for a longer time, hence to reach longer runout distances.

However, hindered settling requires that the debris pores be filled with air at or close to lithostatic pressure. It is unlikely that initial air pore pressure within the failing mass is more than atmospheric, so, in order to fill all the pores with air at lithostatic pressure, a large volume of air should be incorporated rapidly during the falling stage. The volume of atmospheric air that should be incorporated (V_a) is the product of the volume of the landslide (V), its porosity ($1-C$) and its average lithostatic pressure ($\rho_b gh/2$) divided by the atmospheric pressure (P_a),

$$V_a = V(1-C)\frac{\rho_b gh}{2P_a}. \quad (25)$$

Thick landslides would have to incorporate and pressurise a volume of atmospheric air several times to several tens of times their own volume, a condition difficult to attain. Therefore, although it cannot be ruled out that fluidisation by air may play some role in reducing friction in some landslides, it is probably not the principal mechanism that allows their long runout, particularly for large ones. On Mars, where atmospheric pressure is 100 times less than on the Earth and gravity acceleration only 2.5 less, fluidisation by air would be even more difficult to achieve.

Continuous injection of air at the head base is also unlikely. Mohrig et al. (1998) showed that this could occur for water in submarine debris flows, when the value of the dynamic pressure at the head ($\rho_f U^2/2$) approaches that of static pressure ($[\rho_b - \rho_f]gh$). With air, this condition seems impossible to achieve, even for thin and fast landslides.

Hsü (1975) proposed that, on the airless Moon, dust might constitute the interstitial fluidising phase. It is however difficult to conceive how fine particles may form a suspension in the vacuum. The clouds of dust visible during the landing of the Apollo crafts to which Hsü alludes were most probably caused by the gas jet from the crafts themselves. In the absence of gas, all particles should follow ballistic trajectories and fall at the same velocities whatever their size. The buoyancy that particles feel in a fluid or suspension fluid is due to the static pressure gradient existing in the fluid. Even if a theoretical bulk density can be calculated for a "suspension" in vacuum, there can be no pressure gradient, so no buoyancy effect. Therefore, in the absence of externally derived fluids, such as those that would be produced during a meteorite impact, fluidisation is not possible on the Moon.

4.5. Fluidisation by water

The main difference between landslides and debris flows relevant to their rheology is probably that debris flows are saturated with water while landslides are not. Debris flows are typically much more mobile than landslides of the same volume and this difference is largely attributed to the abundance of water in the formers (Iverson, 1997). Water is thought to lower granular friction through the occurrence of high pore pressure gradients. By opposition to the obviously "wet" debris flows, landslides have sometimes been described as "dry". It is nevertheless well known that there are not two clearly separated types of flow, some totally dry and the others fully saturated with water. Instead, there must be a continuum of water saturation between hypothetical dry landslides and saturated debris flows.

There is good evidence that landslides can transform into debris flows (e.g., Plafker and Ericksen, 1978; Voight et al., 1983; Iverson et al., 1997; Vallance and Scott, 1997; Mothes et al., 1998; Takarada et al., 1999), which demonstrates that there is a continuum of water saturation and that deposits which still have characteristics typical of landslides can form from mass flows containing some water. A substantial amount of water is likely to be already present in the failing mass of most landslides. This is, for example, the case of most landslides in New Zealand, which nevertheless produce typical hummocky deposits containing shattered megablocks with jigsaw fractures (Palmer et al., 1991). The presence of a water table is often a necessary condition to trigger mass collapse by an increase in pore water pressure under undrained conditions (e.g., Iverson, 1997). Water can further be added to the base of landslides by incorporation of saturated valley sediments or directly by mixing with water from a river. Clastic dykes of fine material injected from the base were found in the deposits of the Blackhawk landslide (Johnson, 1978) and the Arequipa volcanic landslide (Legros et al., 2000), suggesting the presence of a high-fluidity, muddy basal layer (Fig. 7). The matrix of the freshly deposited, 1984 Ontake-san landslide was also described as wet (Voight and Sousa, 1994). Submarine landslides must contain water and, nevertheless, they leave deposits with a morphology distinctive from that of saturated debris-flow deposits. As discussed above, ground ice is also likely to be present in most Martian landslides. Therefore, there is good evidence that most landslides contain some water. As we know that water enhances the mobility of debris flows, a logical hypothesis is that it can also enhance the mobility of landslides. Water would reduce granular friction through the development of high pore pressure, essentially like in saturated debris flows, except that in landslides, only a part of the flow, typically the base, would be saturated in water.

Compared to air, water presents several advantages for developing and maintaining high pore pressures: it is denser, incompressible and more viscous. The density of water ensures a minimum (hydrostatic) pore pressure gradient of 10^4 Pa m^{-1}, which can already account for a significant reduction of the granular shear stress, as shown by Eq. (22). The incompressibility of water allows it to be easily loaded by the debris and attain lithostatic pressure with a negligible volume contraction. Thus, large landslides need not incorporate huge volumes of water in order to be fluidised, as is necessary with air fluidisation. Water initially present in the failing mass is sufficient. For any given pressure gradient and permeability, the higher viscosity of water compared to that of air reduces its rate of escape by a factor of 100 (Eq. (1)). In addition, the process of aggregative fluidisation during which air is passed through the sediment bed in the form of bubbles, and which dramatically decreases the effective permeability of the bed, does not occur with water (Wilson 1984). Therefore, water seems to be a fluid much more appropriate than air for partial fluidisation of landslides. Recent experimental and theoretical work by Major and Iverson (1999), Major (2000), and Iverson

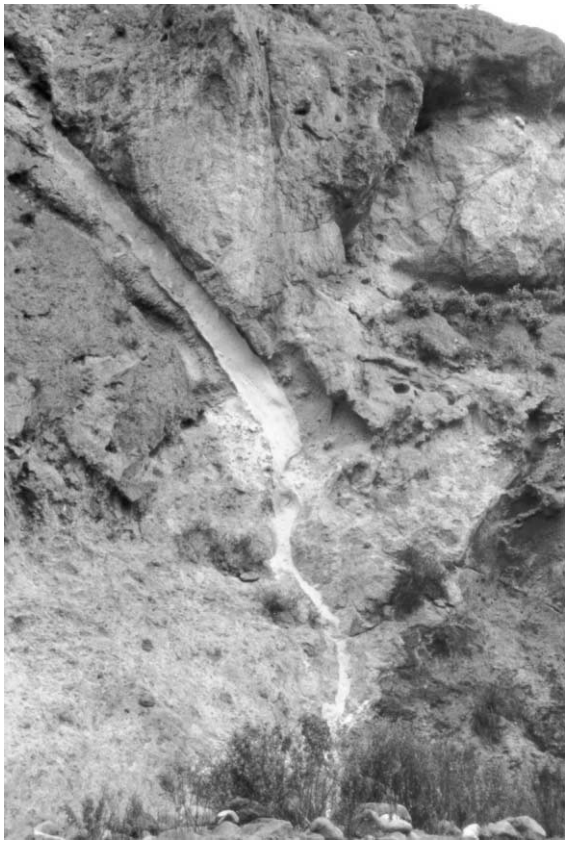

Fig. 7. Photograph of a 20-m-high clastic dyke of muddy sediment injected into the Arequipa volcanic landslide deposit.

and Denlinger (2001) has shown that high pore-water pressures, nearly sufficient to cause liquefaction, could be maintained during debris-flow emplacement.

As there is probably not a continuous supply of water at the bottom of landslides, maintaining high pore pressures requires a net downward movement of the debris, which implies some kind of progressive deposition at the base (Iverson, 1997). It is unlikely, however, that the deposit forms by progressive aggradation up to the top. The hummocky topography of landslide deposits rather suggests a deposition en masse due to the strength of the debris. A high strength is indeed expected in the upper, unsaturated part of landslides. Therefore, the unsaturated upper part would account for the very irregular surface of landslide deposits, contrasting with the smoother surface of saturated debris-flow deposits, while the saturated base would account for the long runout, unexpected for dry granular debris. All other things being equal, runout should be a positive function of the saturated volume, which can explain the higher mobility of larger landslides. This view is consistent with the fact that saturated debris flows, in which the fluid phase is believed to be responsible for the long runout, show an increase of runout with volume similar to that of landslides (Fig. 3b; Table 3).

5. Velocity of landslides

The degree to which topography controls emplacement of landslides primarily depends on their velocity and can serve to constrain rheological models. The relationship between velocity and topography can be described using the "energy line" concept (Sheridan, 1979). The energy line defines the maximum height that a landslide would be able to reach by converting all its kinetic energy into potential energy, as a function of the distance away from the origin. Note that, with this definition, the energy line does not represent the total mechanical energy of the landslide, but rather the mechanical energy by mass unit. This

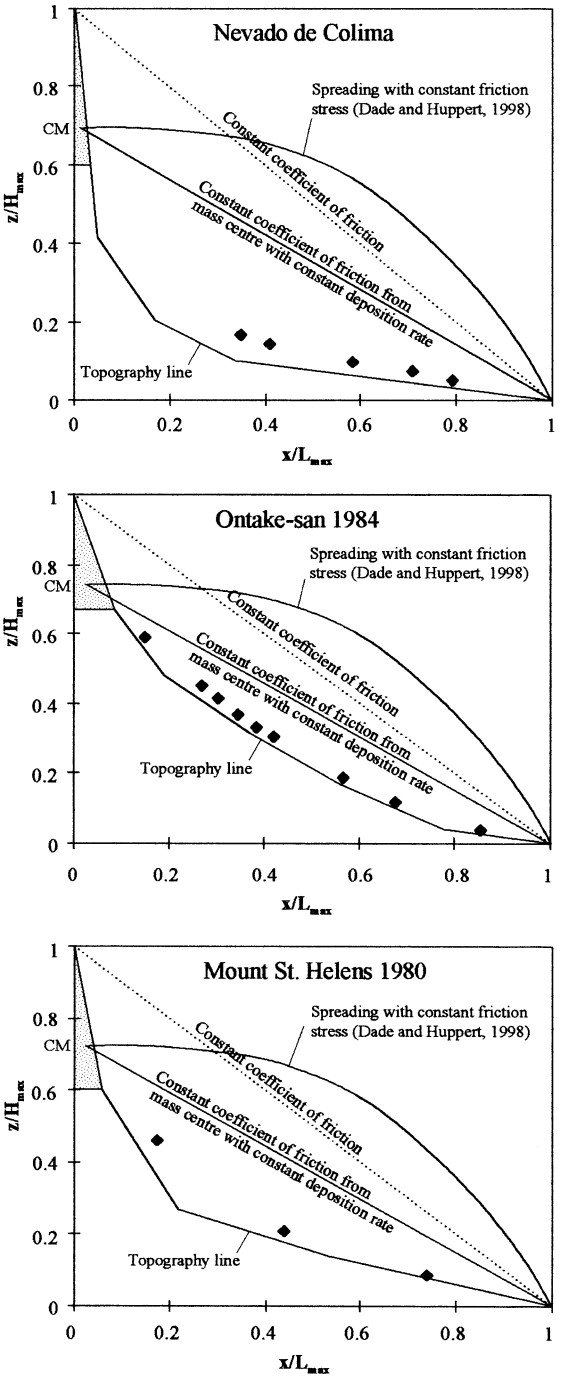

Fig. 8. Energy lines for models which assume a constant friction stress or a constant coefficient of friction, compared with data from natural landslides (solid diamonds). The velocities inferred for the three landslides are small (diamonds close to the topography line) and tend to decrease downstream. The models are seen to overestimates velocities. Vertical and horizontal coordinates, z and x, are normalised to H_{max} and L_{max}, respectively. Shaded area represents the failing mass and CM is the centre of mass.

definition is convenient because, as the mass of landslides may change during transport, the parameter that can be estimated is velocity, not mechanical energy. Although the energy line concept has been much used with constant coefficients of friction, thus producing straight energy lines, it can be used with other rheological models.

There are few landslides for which reliable velocity estimates are available. Fig. 8 shows the data for the Mount St. Helens (Voight et al., 1983), the Nevado de Colima (Stoopes and Sheridan, 1992) and the Ontake-san (Voight and Sousa, 1994) landslides, together with the energy lines predicted by various models. It appears that the actual landslide velocities are always much lower than predicted by models which assume a constant coefficient of friction. These include models in which energy is dissipated by solid friction at the base of a sliding block or by frictional or collisional particle interactions within a granular debris. According to these models, landslides should be much less controlled by topography than they are. This was also noted by McEwen and Malin (1989) and Voight and Sousa (1994) from their numerical simulations of, respectively the Mount St. Helens and the Ontake-san landslides. One reason for this is that energy lines have been drawn from the top of the failing mass, whereas they should start from its centre of mass. Fig. 8 also shows energy lines starting from the centre of the failing mass and corresponding to a constant coefficient of friction, with a constant loss of mass by unit distance. As shown by Eq. (8), when a landslide loses mass by deposition, it decelerates less rapidly and the slope of the energy line decreases. Although these energy lines are much lower than those starting from the top of the failing mass, they still predict velocities much greater than those estimated for the three landslides. Moreover, these energy lines are based on the assumption that the rate of mass loss does not vary with distance, while the deposits of the three landslides are actually wider and thicker near source. The energy lines corresponding to such mass distributions would be convex curves always above the straight lines presented, so they would predict still greater velocities. Therefore, models which assume a constant coefficient of friction tend to overestimate landslide velocity, even when mass loss by deposition is taken into account.

Dade and Huppert (1998) recently proposed a physical model for landslide transport which predicts a correlation between volume and area deposit in good agreement with existing data. The model assumes a constant dissipative stress. This is different from the traditional assumption of constant *coefficient* of friction. For a slide that has a constant coefficient of friction, the loss of energy by unit mass and unit distance travelled is constant (Eq. (8)), which gives the typical straight energy line. For a landslide with a constant dissipative stress (τ_s), the loss of energy by unit distance is

$$\frac{dE}{dx} = -\tau_s A. \tag{26}$$

If the area (A) is constant, we get a straight energy line but if the landslide is spreading, A increases with x and so does the force acting against the movement, dE/dx. Assuming that $A = \lambda x^2$ (Dade and Huppert, 1998), where 2λ is the angular extent of the assumed uniform sector through which the landslide spreads, and integrating Eq. (26) yields the form of the relation between mechanical energy and distance from the origin,

$$E = E_0\left(1 - \frac{x^3}{L_{max}^3}\right). \tag{27}$$

Fig. 8 shows that this gives energy lines still higher than for the model of constant coefficient of friction. Thus, this model predicts velocities which are much too high compared with those of real landslides.

In the numerical simulations of Campbell et al. (1995), the velocity is seen to increase nearly linearly with time along the initial slope and then to decrease nearly linearly over the flat, except near the end of transport where deceleration lowers. The roughly constant acceleration and deceleration suggest a constant coefficient of friction, and the maximum velocity at the foot of the initial slope is about that expected for a straight energy line model.

The relatively low velocities of natural landslides suggest that they are submitted to velocity-dependent drag forces. High velocities acquired during the

initial falling stage would therefore be rapidly dissipated. Landslides would then go on with little help from their initial kinetic energy. In these conditions, their ability to spread on gentle slopes implies that the granular friction coefficient is very low and that landslides flow rather than slide. Velocity would primarily be controlled by the local slope and depth of the flow, as it appears to occur for debris flows (Pierson, 1985). The downstream decrease in velocity would thus be explained by the decrease of flow depth with distance, due to spreading and deposition, as well as by the common decrease in slope gradient away from source. The flow would progressively lose mass by deposition and travel until it runs out of material.

6. Self-similar shape of landslide deposits

Velocity data from landslides suggest that they rapidly lose the kinetic energy gained on the initial slope and that their spreading is mainly controlled by their volume and the local slope. This means that the part of a landslide which passes beyond a certain distance will spread somehow independently of the rest. In other words, the volume passing beyond a certain distance does not "know" that it is part of a larger landslide, and spreads as if it was an independent landslide. One would therefore expect that the correlation observed between volumes and areas of landslide deposits be also valid for portions of individual deposits. This means that, for a given landslide, the volume which has passed a certain distance should always be correlated with the area of the deposit beyond that distance. As noted by several authors (Hungr, 1990a; Vallance and Scott, 1997; Iverson et al., 1998; Dade and Huppert, 1998) and in Fig. 3e, the area covered by landslide and debris-flow deposits is about proportional to their volume at the power two thirds, $A \sim cV^{2/3}$. We may calculate the self-similar shape of the deposit for which A_x is always equal to $cV_x^{2/3}$, where A_x and V_x are the area and volume of the deposit beyond a distance x from the origin. On a real, irregular topography, such a calculation may be very

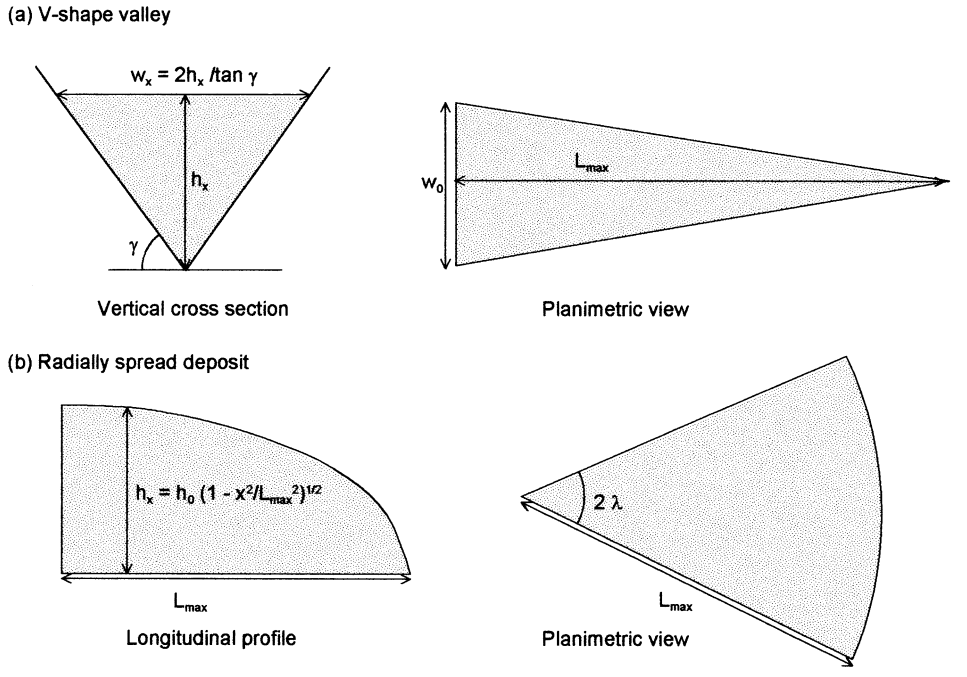

Fig. 9. Sketch of the self-similar shape of landslide deposits, and definition of the variables used in the text and the appendix: (a) in a V-shape valley; (b) radially spread deposit.

complex, but we can use idealised geometrical cases. One particularly relevant geometry is that of a *V*-shape valley channelling the landslide (Fig. 9a). Such a valley is characterised by the slope of its sides, γ. At a given distance x from the origin, the deposit has a thickness h_x at the centre of the valley and a width $w_x = 2h_x/\tan\gamma$. It can be demonstrated (Appendix A) that $A_x = cV_x^{2/3}$ for any x if the thickness of the deposit decreases linearly away from the origin, following the equation

$$h_x = h_0\left(1 - \frac{x}{L_{\max}}\right), \tag{28}$$

where $h_0 = 3V_0/A_0$.

Data of thickness versus distance from the origin are scarce for landslide deposits. The large volcanic landslide of Mount Shasta was emplaced in a wide, open valley, and has a volume and an area estimated to 45 km^3 and 675 km^2, respectively (Crandell, 1988). Crandell divided the deposit into seven areas labelled from A to G, situated at increasing distances from Shasta volcano, except for area F which is a narrow marginal band elongated in the valley direction. For each area, he provided an estimate of the volume. Based on these data, Fig. 10a shows the relation between the volume and the area found beyond a certain distance. It can be seen that the relation $A \sim 50V^{2/3}$ found for the whole deposit is also approximately valid all along the deposit. Assuming that the deposit has a geometry roughly of the type schematically represented in Fig. 9a, with $L_{\max} \sim 55$ km and $x_0 \sim 10$ km, the central thickness must vary according to Eq. (28) with $h_0 \sim 200$ m. This is in rough agreement with Crandell's maximum thickness estimates (Fig. 10b).

Voight et al. (1983) showed that the Mount St. Helens landslide was emplaced in three blocks. Block 3 was able to flow in the Toutle River valley for some 20 km. The deposit has a wedge shape for which both the central thickness and the width in the Toutle River valley are observed to decrease roughly linearly with distance from the origin. A roughly linear decrease of the thickness is also observed for the deposit of the Elm landslide in the Unterthal valley (Hsü, 1975). For a landslide spreading over an angular sector (Fig. 9b), the thickness is not expected to vary much with distance from the origin (Appendix B), which is in agreement with the thickness profile of the Sherman

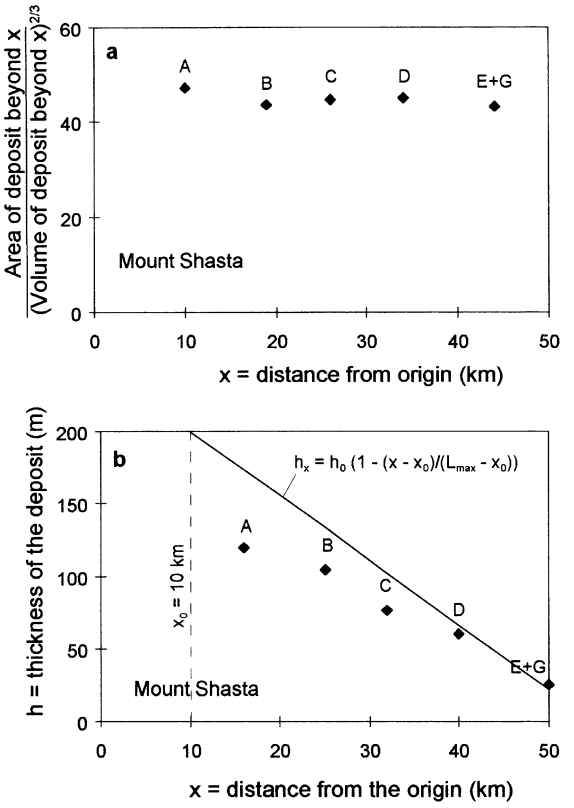

Fig. 10. (a) Ratio of area of deposit beyond a certain distance to volume of deposit beyond the same distance at the power two-thirds, for the Shasta volcanic landslide. The ratio is roughly constant. (b) Thickness profile predicted if the deposit has the shape represented in Fig. 9a (solid line), compared with the maximum thickness observed (solid diamonds). Capital letters refer to the divisions of Crandell (1988). Zone F is not used as it is a marginal, elongated band parallel to the valley direction.

landslide deposit (McSaveney, 1978). In detail, discrepancies between the idealised geometrical model and natural landslide deposits are expected, because of the irregular geometry of natural valleys, and the possible evolution of the rheology of landslides as they progress downstream (e.g., Voight and Sousa, 1994). More detailed data on the distribution of mass of landslide deposits as a function of the topography are needed. The trend observed in the examples presented above nevertheless reinforces the idea explored in a previous section that the area and the runout distance of a landslide deposit primarily depend on its volume, and that the fall height is probably of secondary importance.

7. Conclusions

The present examination and discussion of several issues relevant to landslide mobility allows the following conclusions to be proposed.

(1) The ratio of the height lost to the distance travelled by the centre of mass of landslides, H/L, is generally much lower than the coefficient of friction of normal rocks, μ. The reduction of the apparent coefficient of friction of landslides is real and is not an artefact due to the fact that the ratio of maximum fall height to maximum runout distance, H_{max}/L_{max} is commonly used instead of H/L. In many cases, H_{max}/L_{max} is probably not much smaller than H/L.

(2) Current understanding of granular avalanches suggests that they exhibit a constant coefficient of friction, close to the coefficient of friction of their particles, in both the frictional, quasistatic flow regime and the collisional, rapid flow regime. In these conditions, it has been shown here that, even if the avalanche can spread by progressive deposition, so as to increase L_{max}, the ratio H/L remains equal to μ. A fluid-absent, granular model is therefore unable to explain landslide mobility, unless granular friction is significantly reduced by high pore-fluid pressure or the assumption of a constant coefficient of friction breaks down. The latter possibility has been proposed by Campbell et al. (1995) to explain the results of numerical simulations that were in a regime transitional between frictional and collisional. This transitional regime is still poorly understood and to what extent the results of the simulations are applicable to real granular systems is unknown. Whether fluid-absent, granular avalanches can explain the long runout of landslides is still an unresolved question.

(3) The effective coefficient of friction can be significantly reduced by the presence of an interstitial fluid which partly supports the granular load, and thus lowers the granular stress. The fluid would also add a velocity-dependent, viscous stress. Models which use a constant coefficient of friction predict velocities that are much greater than those inferred for real landslides and cannot account for their great responsivity to topography. The low velocities of landslides suggest that they behave much like a fluid, with a velocity-dependent dissipative stress and a low effective coefficient of solid friction, in agreement with what is expected for partly fluidised debris.

(4) The ratio H/L may therefore be physically meaningless. The good correlations between runout distance and volume, and area and volume, suggest that landslide spreading is essentially controlled by their own volume, and not by H.

(5) Martian and lunar landslides are not evidence that landslides can travel large distances as fluid-absent, granular systems. Martian landslides are likely to contain substantial amounts of ground ice, part of which could melt owing to frictional heating during transport. Long-runout landslides are extremely rare on the Moon, and the two examples described in the literature are associated with meteorite impact and may in part have been transported as ballistic ejecta.

(6) Air is unlikely to fluidise landslides efficiently, nor to support them by forming a compressed layer at their base. Fluidisation or basal lubrication by air becomes increasingly difficult as landslide volume increases, so air cannot explain the greater mobility of larger landslides.

(7) Water is much more efficient than air as a fluidising medium, due to its higher density and viscosity, and its incompressibility. Hummocky surfaces and jigsaw fractures are observed in the deposits of landslides which probably contained large amounts of water. Landslides are unsaturated with water, but probably seldom dry. As it is generally admitted that water plays a fundamental role in the large mobility of saturated debris flows, it seems likely that it also plays a role in the dynamics of landslides. The increase in landslide runout with volume follows the same trend as that observed for saturated debris flows, as expected if they share the same physics.

(8) The low velocity of landslides and their inferred fluid-like behaviour suggest that their spreading beyond a certain distance is primarily controlled by the local slope and by the volume that passes that distance, and that there is no ''memory'' of the initial drop height or of the volume of the landslide which does not pass that distance. The relation between volume and area of the deposit beyond any distance should therefore be constant within a given deposit, which allows the shape of the deposit to be predicted for different topographies.

This last point emphasises the need for more detailed data on the areal distribution of the mass of landslide deposits. It also suggests that hazard zonation for landslide events should rely on their area–

volume relationship, as recently proposed for debris flows (Iverson et al., 1998), rather than on their apparent coefficient of friction, often used for this type of effort.

Acknowledgements

Richard Iverson and an anonymous reviewer provided constructive reviews. The author is supported by a TMR contract (ERBFMBICT983445).

Appendix A. Self-similar shape of a landslide deposit in a V-shape valley

We are looking for the shape of a deposit in a V-shape valley such that $A_x = cV_x^{2/3}$ for any x, where x is the distance from the origin, A_x and V_x are, respectively, the area and the volume of the deposit beyond distance x, and $c = A_0/V_0^{2/3}$ is a constant, where the subscript 0 refers to the origin of x. The deposit is defined by its thickness at the centreline of the valley, h_x, its width at the top, w_x, and its total length, L_{max}. These parameters are schematically represented in Fig. 9a, together with γ, the angle of the valley sides with the horizontal. (Note that for simplicity this assumes that there is no distance x_0 between the source and the proximal end of the deposit. If there is a certain x_0, as in Fig. 1, one should use $x - x_0$ instead of x, and $L_{max} - x_0$ instead of L_{max} in the following equations). From Fig. 9a, we see that

$$w_x = \frac{2h_x}{\tan\gamma}. \tag{A1.1}$$

The area of a vertical cross-section in the deposit is defined as

$$S_x = \frac{w_x h_x}{2} = \frac{h_x^2}{\tan\gamma}. \tag{A1.2}$$

Anticipating from dimensional arguments that h_x and w_x will both vary linearly with x, we propose the following expression for h_x,

$$h_x = h_0\left(1 - \frac{x}{L_{max}}\right). \tag{A1.3}$$

By using the three equations above, we can now calculate A_x and V_x,

$$A_x = \int_x^{L_{max}} w_x \mathrm{d}x = \frac{h_0(L_{max} - x)^2}{L_{max}\tan\gamma}, \tag{A1.4}$$

$$V_x = \int_x^{L_{max}} S_x \mathrm{d}x = \frac{h_0^2(L_{max} - x)^3}{3L_{max}^2\tan\gamma}, \tag{A1.5}$$

from which we can check that

$$A_x = \frac{A_0}{V_0^{2/3}} V_x^{2/3}. \tag{A1.6}$$

Appendix B. Self-similar shape of a radially spread landslide deposit

Let us consider a deposit of radial shape over a sector of angle 2λ, and with other parameters defined as in Appendix A and Fig. 9b. We want to find the radial profile of the thickness for which the area beyond a certain distance x is always proportional to the volume beyond this distance at the power two third, as expressed in Eq. (A1.6). We can show that the equation

$$h_x = h_0\left(1 - \frac{x^2}{L_{max}^2}\right)^{\frac{1}{2}} \tag{A2.1}$$

satisfies this condition. The area and the volume beyond x are, respectively, given by

$$A_x = \int_x^{L_{max}} 2\lambda x \mathrm{d}x = \lambda(L_{max}^2 - x^2) = A_0\frac{(L_{max}^2 - x^2)}{L_{max}^2} \tag{A2.2}$$

$$V_x = \int_x^{L_{max}} h_x 2\lambda x \mathrm{d}x = \frac{2h_0\lambda}{3L_{max}}(L_{max}^2 - x^2)^{\frac{3}{2}} = V_0\left(\frac{L_{max}^2 - x^2}{L_{max}^2}\right)^{\frac{3}{2}} \tag{A2.3}$$

from which Eq. (A1.6) is verified.

References

Bagnold, R.A., 1954. Experiments on a gravity-free dispersion of large solid spheres in a Newtonian fluid under shear. R. Soc. London, Proc. 225, 49–63.

Battaglia, M., 1993. On pyroclastic flow emplacement. J. Geophys. Res. 98, 22269–22272.

Campbell, C.S., 1989. Self-lubrication for long runout landslides. J. Geol. 97, 653–665.

Campbell, C.S., 1990. Rapid granular flows. Annu. Rev. Fluid Mech. 22, 57–92.

Campbell, C.S., Cleary, P.W., Hopkins, M., 1995. Large-scale landslide simulations: global deformation, velocities and basal friction. J. Geophys. Res. 100, 8267–8273.

Cannon, S.H., Savage, W.Z., 1988. A mass-change model for the estimation of debris-flow runout. J. Geol. 96, 221–227.

Cleary, P.W., Campbell, C.S., 1993. Self-lubrication for long-runout landslides: examination by computer simulations. J. Geophys. Res. 98, 21911–21924.

Crandell, D.R., 1988. Gigantic debris avalanche of Pleistocene age from ancestral Mount Shasta volcano, California, and debris-avalanche hazard zonation. U.S. Geol. Surv. Bull. 1861, 29 pp.

Dade, W.B., Huppert, H.E., 1998. Long-runout rockfalls. Geology 26, 803–806.

Davies, T.R.H., 1982. Spreading of rock avalanche debris by mechanical fluidization. Rock Mech. 15, 9–24.

Davies, T.R.H., McSaveney, M.J., 1999. Runout of dry granular avalanches. Can. Geotech. J. 36, 313–320.

Drake, T.G., 1990. Structural features in granular flows. J. Geophys. Res. 95, 8681–8696.

Druitt, T.H., 1995. Settling behaviour of concentrated, poorly sorted dispersions and some volcanological applications. J. Volcanol. Geotherm. Res. 65, 27–39.

Erlichson, H., 1991. A mass-change model for the estimation of debris-flow runout, a second discussion: conditions for the application of the rocket equation. J. Geol. 99, 633–634.

Fahnestock, R.K., 1978. Little Tahoma peak rockfalls and avalanches, Mount Rainier, Washington, USA. In: Voight, B. (Ed.), Rockslides and Avalanches. 1. Natural Phenomena. Elsevier, Amsterdam, pp. 181–196.

Goguel, J., 1978. Scale-dependent rockslides mechanisms, with emphasis on the role of pore fluid vaporization. In: Voight, B. (Ed.), Rockslides and Avalanches. 1. Natural Phenomena. Elsevier, Amsterdam, pp. 693–705.

Guest, J.E., 1971. Geology of the farside crater Tsiolkovsky. In: Fieder, G. (Ed.), Geology and Physics of the Moon. Elsevier, Amsterdam, pp. 93–103.

Hampton, M.A., Lee, H.J., Locat, J., 1996. Submarine landslides. Rev. Geophys. 34, 33–59.

Hanes, D.M., Inman, D.L., 1985. Experimental evaluation of a dynamic yield criterion for granular fluid flows. J. Geophys. Res. 90, 3670–3674.

Hayashi, J.N., Self, S., 1992. A comparison of pyroclastic flow and landslide mobility. J. Geophys. Res. 97, 9063–9071.

Hazlett, R.W., Buesch, D., Anderson, J.L., Elan, R., Scandone, R., 1991. Geology, failure conditions, and implications of seismogenic avalanches of the 1944 eruption at Vesuvius, Italy. J. Volcanol. Geotherm. Res. 47, 249–264.

Heim, A., 1932. Bergsturz und Menschenleben. Fretz und Wasmuth, Zürich, p. 218.

Howard, K.E., 1973. Avalanche mode of motion: implications from lunar examples. Science 180, 1052–1055.

Hsü, K.J., 1975. Catastrophic debris streams (Sturzstroms) generated by rockfalls. Geol. Soc. Am. Bull. 86, 129–140.

Hungr, O., 1990a. Mobility of rock avalanches: report of the National Research Institute of Earth Science and Disaster Prevention, Japan, 46, 11–20.

Hungr, O., 1990b. A mass-change model for the estimation of debris-flow runout: a discussion. J. Geol. 98, 791.

Hungr, O., Evans, S.G., 1997. A dynamic model for landslides with changing mass. Eng. Geol. Environ. 41, 719–722.

Hungr, O., Morgenstern, N.R., 1984a. Experiments on the flow behaviour of granular materials at high velocity in an open channel. Geotechnique 34, 405–413.

Hungr, O., Morgenstern, N.R., 1984b. High-velocity ring shear test on sand. Geotechnique 34, 415–421.

Iverson, R.M., 1997. The physics of debris flows. Rev. Geophys. 35, 245–296.

Iverson, R.M., Denlinger, R.P., 2001. Flow of variably fluidized granular masses across three-dimensional terrain: 1. Coulomb mixture theory. J. Geophys. Res. 106, 537–552.

Iverson, R.M., Reid, M.E., Lahusen, R.G., 1997. Debris-flow mobilization from landslides. Annu. Rev. Earth Planet. Sci. 25, 85–138.

Iverson, R.M., Schilling, S.P., Vallance, J.W., 1998. Objective delineation of lahar-inundation hazard zones. Geol. Soc. Am. Bull. 110, 972–984.

Johnson, A.M., 1970. Physical Processes in Geology. Freeman, San Francisco, p. 577.

Johnson, B., 1978. Blackhawk landslide, California, U.S.A. In: Voight, B. (Ed.), Rockslides and Avalanches. 1. Natural Phenomena. Elsevier, Amsterdam, pp. 481–504.

Kent, P.E., 1966. The transport mechanism in catastrophic rock falls. J. Geol. 74, 79–83.

Legros, F., Cantagrel, J.-M., Devouard, B., 2000. Pseudotachylyte (frictionite) at the base of the Arequipa volcanic landslide deposit (Peru) and implications for emplacement mechanisms. J. Geol. 108, 601–611.

Lipman, P.W., Normark, W.R., Moore, J.G., Wilson, J.B., Gutmacher, C.E., 1988. The giant submarine Alika debris slide, Mauna Loa, Hawaii. J. Geophys. Res. 93, 4279–4299.

Lucchitta, B.K., 1977. Crater clusters and light mantle at the Apollo 17 site; a result of secondary impact from Tycho. Icarus 30, 80–96.

Lucchitta, B.K., 1978. A large landslide on Mars. Geol. Soc. Am. Bull. 89, 1601–1609.

Lucchitta, B.K., 1979. Landslides in Valles Marineris, Mars. J. Geophys. Res. 84, 8097–8113.

Lucchitta, B.K., 1987. Valles Marinaris, Mars: wet debris flows and ground ice. Icarus 72, 411–429.

Major, J.J., 2000. Gravity-driven consolidation of granular slurries: implications for debris-flow deposition and deposit characteristics. J. Sediment. Res. 70, 64–83.

Major, J.J., Iverson, R.M., 1999. Debris-flow deposition: effects of pore-fluid pressure and friction concentrated at flow margins. Geol. Soc. Am. Bull. 111, 1424–1434.

McEwen, A.S., 1989. Mobility of large rock avalanches: evidence from Valles Marineris, Mars. Geology 17, 1111–1114.

McEwen, A.S., Malin, M.C., 1989. Dynamics of Mount St. Helens 1980 pyroclastic flows, rockslide-avalanche, lahars and blast. J. Volcanol. Geotherm. Res. 37, 205–231.

McSaveney, M.J., 1978. Sherman Glacier rock avalanche, Alaska, USA. In: Voight, B. (Ed.), Rockslides and Avalanches. 1. Natural Phenomena. Elsevier, Amsterdam, pp. 197–258.

Melosh, H.J., 1979. Acoustic fluidization — a new geologic process? J. Geophys. Res. 84, 7513–7520.

Mills, P., Loggia, D., Tixier, M., 1999. Model for a stationary dense granular flow along an inclined wall. Europhys. Lett. 45, 733–738.

Mohrig, D., Whipple, K.X., Hondzo, M., Ellis, C., Parker, G., 1998. Hydroplaning of subaqueous debris flows. Geol. Soc. Am. Bull. 110, 387–394.

Moore, J.G., Normark, W.R., Holcomb, R.T., 1994. Giant Hawaiian landslides. Annu. Rev. Earth Sci. 22, 119–144.

Mothes, P.A., Hall, M.L., Janda, R.J., 1998. The enormous Chillos Valley Lahar: an ash-flow-generated debris flow from Cotopaxi Volcano, Ecuador. Bull. Volcanol. 59, 233–244.

Naranjo, J.A., Francis, P.W., 1987. High velocity debris avalanche at Lastarria volcano in the north Chilean Andes. Bull. Volcanol. 49, 509–514.

Norem, H., Locat, L., Schieldrop, B., 1990. An approach to the physics and the modeling of submarine flowslides. Mar. Geotechnol. 9, 93–111.

Palmer, B.A., Alloway, B.V., Neall, V.E., 1991. Volcanic-debris-avalanche deposits in New-Zealand: lithofacies organisation in unconfined, wet-avalanche flows. Sedimentation in volcanic settings. SEPM Spec. Publ. 45, 89–98.

Plafker, G., Ericksen, G.E., 1978. Nevados Huascarán avalanches, Peru. In: Voight, B. (Ed.), Rockslides and Avalanches. 1. Natural Phenomena. Elsevier, Amsterdam, pp. 277–314.

Pierson, T.C., 1985. Initiation and flow behaviour of the 1980 Pine Creek and Muddy River lahars, Mount St. Helens, Washington. Geol. Soc. Am. Bull. 96, 1056–1069.

Pierson, T.C., Janda, R.J., Thouret, J.-C., Borrero, C.A., 1990. Perturbation and melting of snow and ice by the 13 November 1985 eruption of Nevado del Ruiz, colombia, and consequent mobilisation, flow and depostion of lahars. J. Volcanol. Geotherm. Res. 41, 17–66.

Savage, S.B., Hutter, K., 1989. The motion of a finite mass of granular material down a rough incline. J. Fluid Mech. 199, 177–215.

Shaller, P.J., Smith-Shaller, A., 1996. Review of proposed mechanisms for Sturzstroms (long-runout landslides). In: Abott, P.L., Semour, D.C. (Eds.), Sturzstroms and Detachment Faults, Anbza-Boreego Desert State Park, California. South Coast Geol. Soc., Santa Ana, pp. 185–202.

Sheridan, M.F., 1979. Emplacement of pyroclastic flows: a review. In: Chapin, C.E., Elston, W.E. (Eds.), Ash-Flow Tuffs. Geol. Soc. Am., Spec. Pap., vol. 180, pp. 125–136.

Shreve, R.L., 1968a. The Blackhawk landslide. Geol. Soc. Am., Spec. Pap. 108, 1–47.

Shreve, R.L., 1968b. Leakage and fluidisation in air-layer lubricated avalanches. Geol. Soc. Am. Bull. 79, 653–658.

Siebe, C., Komorowski, J.-C., Sheridan, M.F., 1992. Morphology and emplacement of an unusual debris-avalanche deposit at Jocotitlán volcano, Central Mexico. Bull. Volcanol. 54, 573–589.

Siebert, L., 1984. Large volcanic debris avalanches: charcateristics of source areas, deposits, and assiociated eruptions. J. Volcanol. Geotherm. Res. 22, 163–197.

Stoopes, G.R., Sheridan, M.F., 1992. Giant debris avalanches from the Colima Volcanic Complex, Mexico: implications for long-runout landslides (>100 km) and hazard assessment. Geology 20, 299–302.

Straub, S., 1996. Self-organisation in the rapid flow of granular material: evidence for a major flow mechanism. Geol. Rundsch. 85, 85–91.

Straub, S., 1997. Predictability of long runout landslide motion: implications from granular flow mechanics. Geol. Rundsch. 86, 415–425.

Takarada, S., Ui, T., Yamamoto, Y., 1999. Depositional features and transportation mechanism of valley-filling Iwasegawa and Kaida debris avalanches, Japan. Bull. Volcanol. 60, 508–522.

Vallance, J.W., Scott, K.M., 1997. The Osceola Mudflow from Mount Rainier: sedimentology and hazard implications of a huge clay-rich debris flow. Geol. Soc. Am. Bull. 109, 143–163.

Van Gassen, W., Cruden, D.M., 1989. Momentum transfer and the friction in the debris of rock landslides. Can. Geotech. J. 26, 623–628.

Voight, B., Sousa, J., 1994. Lessons from Ontake-san: a comparative analysis of debris avalanche dynamics. Eng. Geol. 38, 261–297.

Voight, B., Janda, R.J., Glicken, H., Douglass, P.M., 1983. Nature and mechanics of the Mount St. Helens rockslide-avalanche of May 1980. Geotechnique 33, 243–273.

Wilson, C.J.N., 1984. The role of fluidisation in the emplacement of pyroclastic flows: 2. Experimental results and their interpretation. J. Volcanol. Geotherm. Res. 20, 55–84.